

1 Supporting information for:

2 **Environment-Sensitivity Functions for Gross Primary Productivity in Light**
3 **Use Efficiency Models**

4 Shanning Bao^{1*}, Thomas Wutzler¹, Sujan Koirala¹, Matthias Cuntz², Andreas Ibrom³, Simon Besnard^{1,4}, Sophia
5 Walther¹, Ladislav Šigut^{1,5}, Alvaro Moreno⁶, Ulrich Weber¹, Georg Wohlfahrt⁷, Jamie Cleverly⁸, Mirco
6 Migliavacca¹, William Woodgate^{9,10}, Lutz Merbold¹¹, Elmar Veenendaal¹², and Nuno Carvalhais^{1,13*}

7 **S1. Relationship between partial sensitivity functions and site-specific properties**

8 To analyze the relationship between the sensitivities of GPP and the site-specific biotic and abiotic traits, we
9 predicted the average partial sensitivity functions and calibrated parameters of the global best model using the
10 site-specific properties collected in section S8. The random forest regression method (Breiman, 2001), which is
11 good at dealing with high-dimensional data and robust to outliers and nonlinear data, was used (regression tree
12 number was 500) to fit each parameter and average partial sensitivity per site according to leave-one-out strategy.
13 In other words, we predicted the parameter or partial sensitivity of the target site ($\text{site}=i$) using the regression
14 model fitted based on all the other sites ($\text{site} \neq i$). To reduce the deviation caused by uncertain parameters, we
15 weighted the model parameters using the reciprocal of parameter uncertainties (defined in section S5).
16 Furthermore, we sorted all the site-specific properties, i.e., predictors, according to the estimated importance by
17 ‘predictorImportance’ tool in MATLAB2019. It defines the sum of mean squared errors reduction due to
18 regression tree splits on every predictor divided by the number of branches as the importance of predictor
19 (Breiman, 2002).

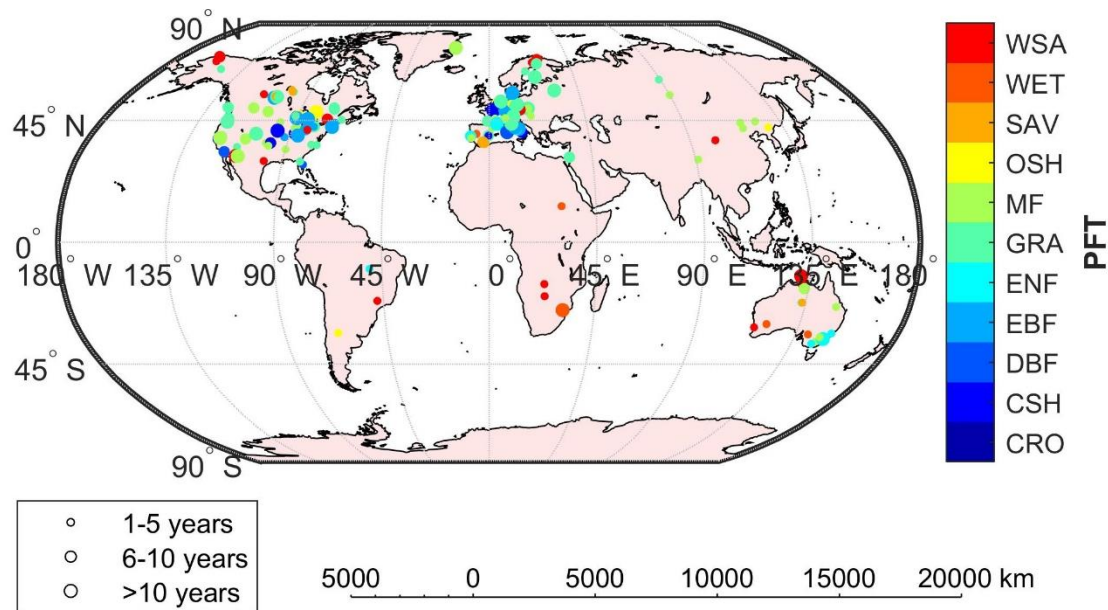
20 The result showed that the average fT , fW could be predicted based on the site-specific properties (Figure S 19).
21 The cross-validated R^2 was 0.56 and 0.44, respectively. According to the predictor importance, the spatial pattern
22 of temperature effect on GPP is mainly related to the climate classification and plant functional types. The soil
23 properties also contribute to some extent. Furthermore, the soil properties were the most critical traits for
24 controlling the spatial pattern of the soil water effect. The climate classification was significant as well. However,
25 the plant functional types and other vegetation traits were not as meaningful as soil properties and climate
26 classification for predicting fW . The $fVPD$, fL and fCI could not be fitted based on currently collected traits. The
27 cross-validated R^2 was all smaller than 0.25.

28 None of the model parameters in the global best model, model #1, could be predicted. The R^2 were all smaller
29 than 0.12. The uncertainties, represented by the standard deviation of the parameters, were considerable in some
30 calibrated parameters (e.g., Figure S 20a). The parameters with considerable uncertainty were typically the
31 outliers in the fitted parameters (e.g., Figure S 20b). The parameter uncertainties were possibly caused by the
32 correlations between the environmental factors and partial sensitivity functions (Figure S 11). To investigate the

33 spatial pattern of model parameters and environmental sensitivities of GPP, it is necessary to reduce the
34 correlated parameters.

35

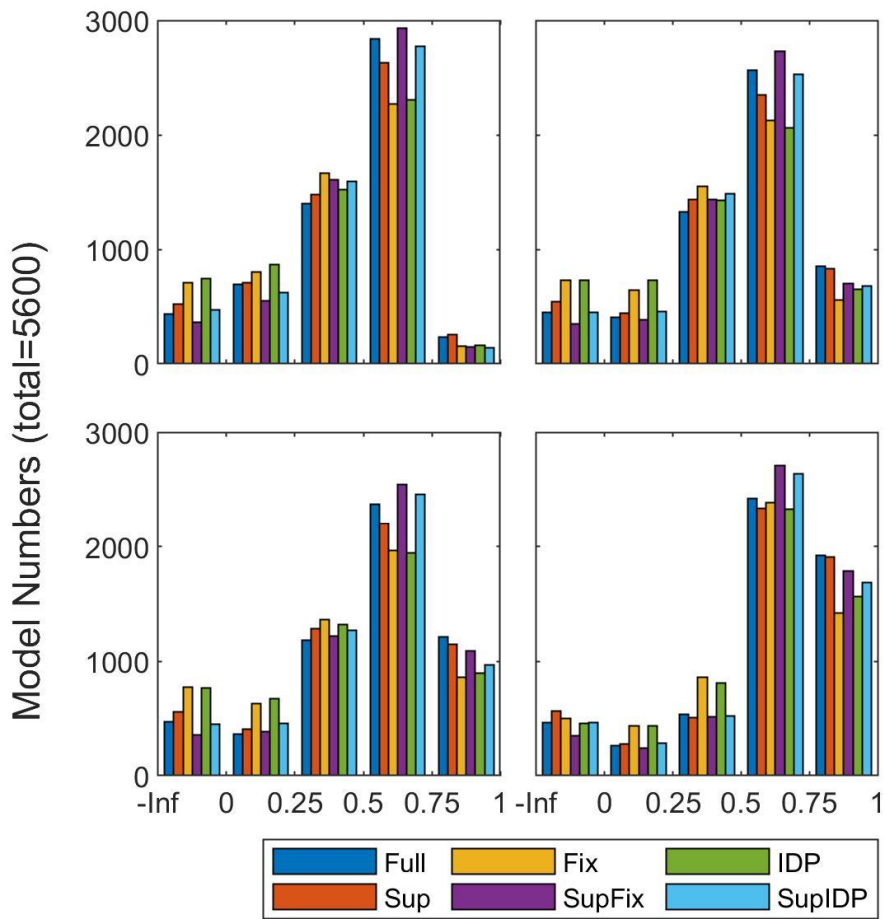
36 **Figures**



37

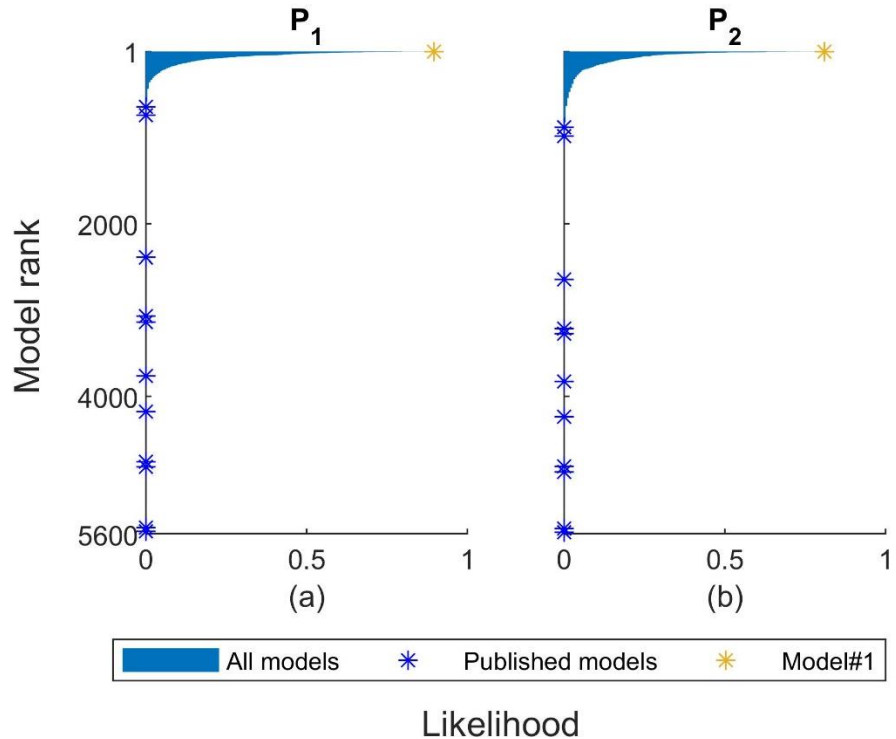
38

Figure S 1. Distribution map of the EC sites (total: 196 sites)



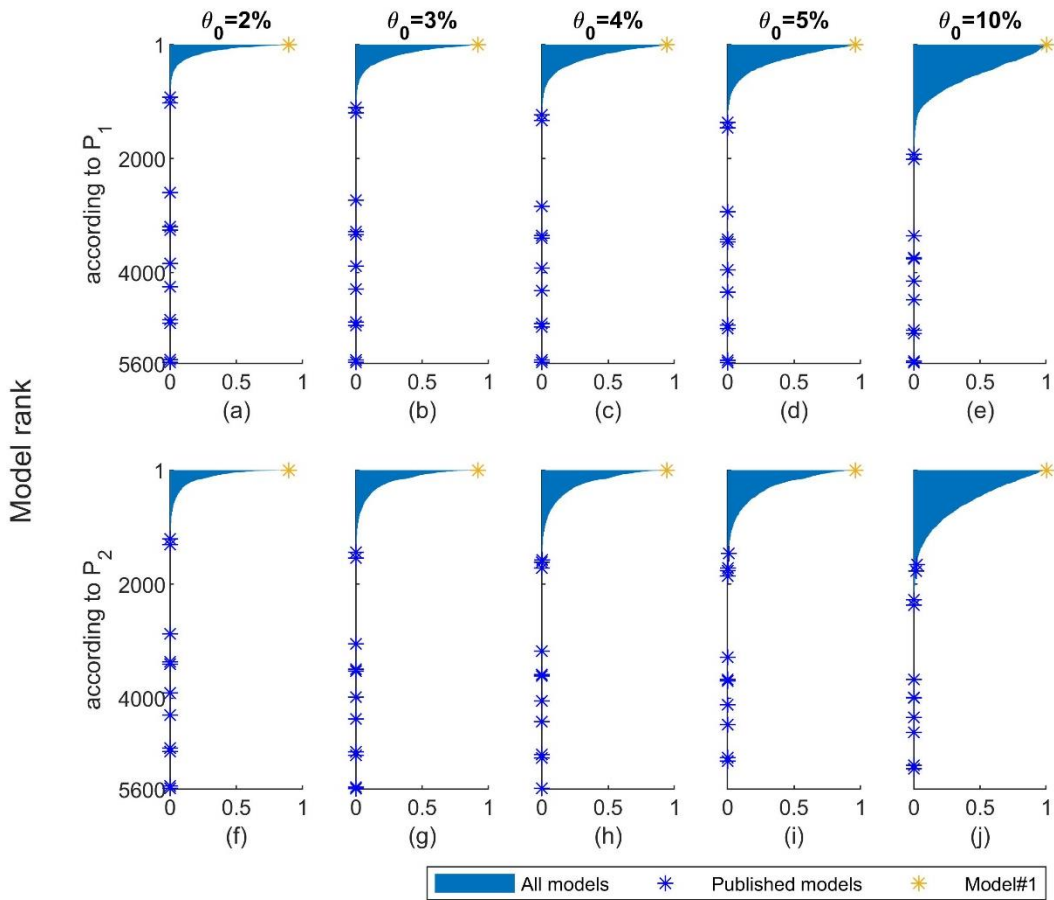
39

40 **Figure S 2. Distribution of global Nash-Sutcliffe model Efficiency (NSE) of different model calibration**
 41 **experiments:** **Full** (optimize the WAI parameters and LUE model parameters jointly under all condition), **Fix**
 42 (fix the WAI parameters and optimize LUE model parameters under all condition), **IDP** (optimize the WAI
 43 parameters independently and optimize LUE model parameters under all condition), **Sup** (optimize the WAI
 44 parameters and LUE model parameters jointly under supply-limited condition), **SupFix** (fix the WAI
 45 parameters and optimize LUE model parameters under supply-limited condition), **SupIDP** (optimize the WAI
 46 parameters independently and optimize LUE model parameters under supply-limited condition)



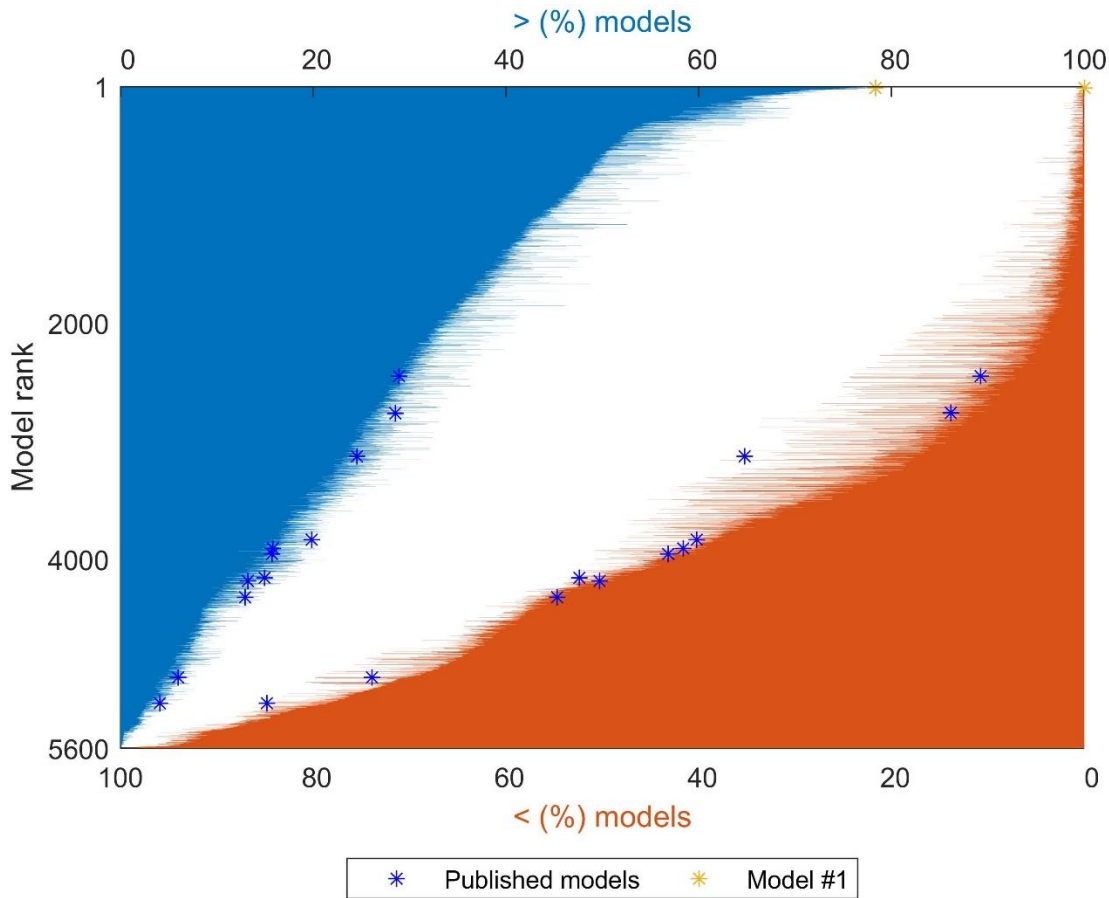
47
48
49
50
51
52

Figure S 3. The likelihoods of all the LUE models using Root Mean Squared Error (RMSE) in the site-sampling method. (a) P_1 represents local goodness of a model for each site-year. (b) P_2 represents overall goodness of a model for all site-years. Yellow asterisk represents the best model selected based on Nash-Sutcliffe model efficiency (model #1), which is also the best model selected based on RMSE. The rankings of Model #1 are the highest according to both P_1 and P_2 .

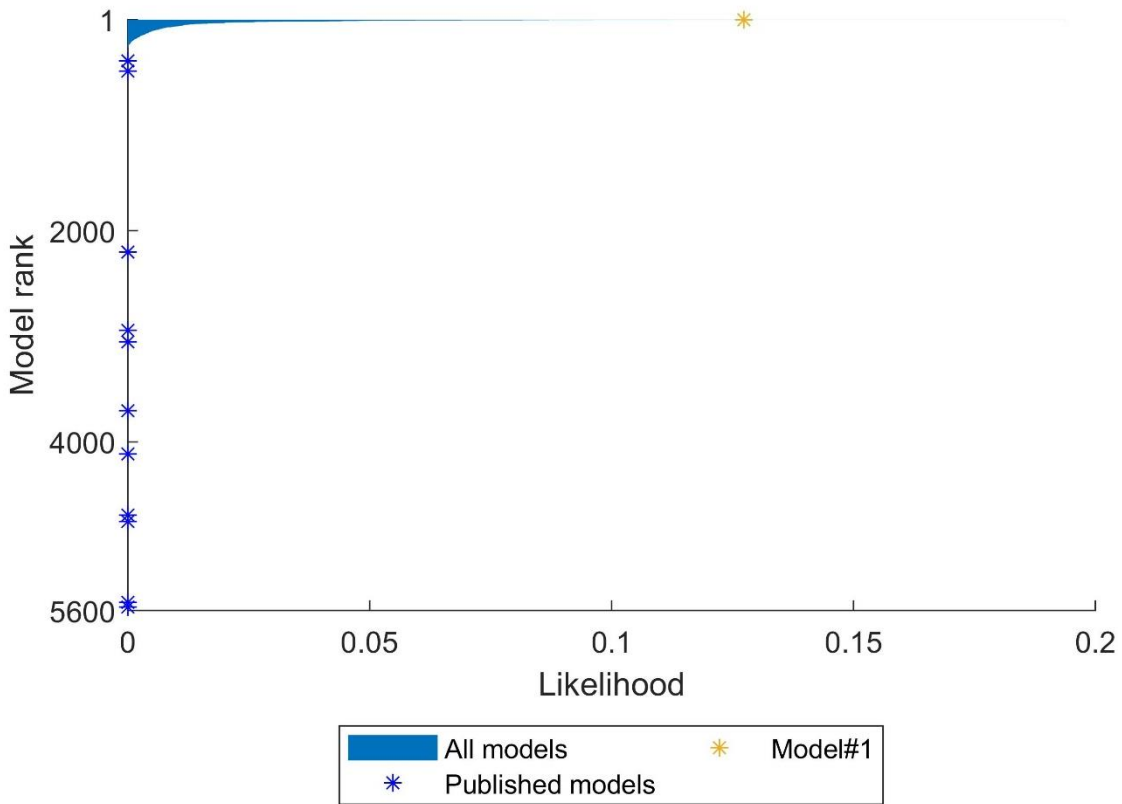


53

54 **Figure S 4. The likelihoods of all the LUE models in the ensemble based on different thresholds (θ_0) to**
 55 **select the best models.** Yellow asterisk is the best model selected according to $\theta_0=1\%$ (model #1), which is
 56 also the best model using $\theta_0=2\%, 3\%, 4\%, 5\%, 10\%$. The rankings of model #1 are higher (i.e., smaller) than
 57 the seventh using different thresholds (a-e) according to P_1 , and are the highest using different thresholds
 58 according to P_2 (f-j). The sum of the rankings of model #1 according to P_1 and P_2 are always the highest. The
 59 likelihoods of published models, represented by blue asterisks, are all zero except when using $\theta_0=10\%$ (j)

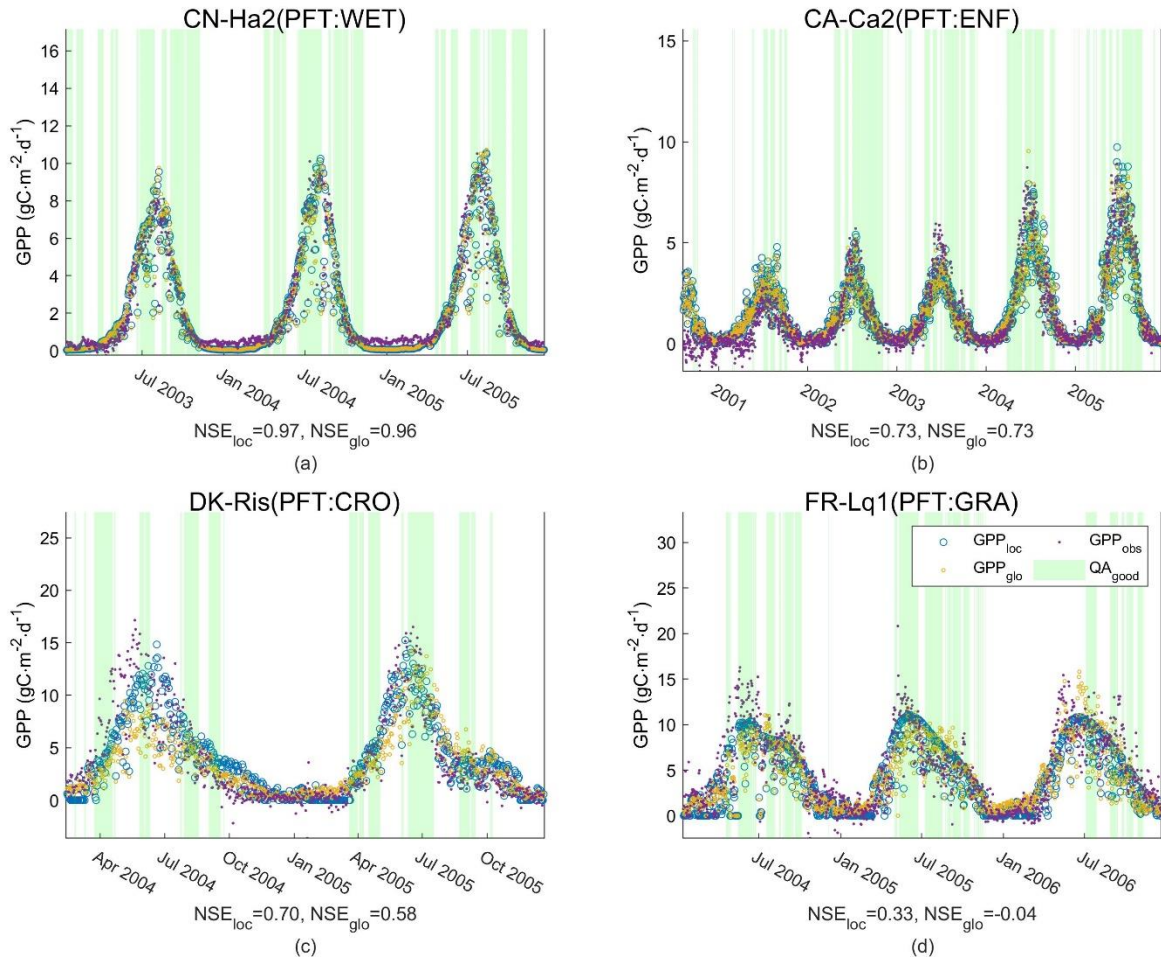


60
61 **Figure S 5. The LUE models sorted according to pair-wise KS hypothesis test, global NSE and spatial**
62 **NSE** (the blue color bar represents the percentage of models than which a model is statistically larger. The
63 white space between blue and orange color represents the percentage of models to which a model is
64 statistically equal. The orange color bar represents the percentage of models than which a model is statistically
65 smaller. The yellow asterisk is the global best model selected according to site-sampling method (model #1),
66 which is the 13th best model here. Blue asterisks are the published model. An example to read the figure is that
67 the global best model is larger than 78% of models, equal to 22% of models and smaller than 0% of models.
68 The percentages are averaged over daily, weekly, monthly and annual scales.)



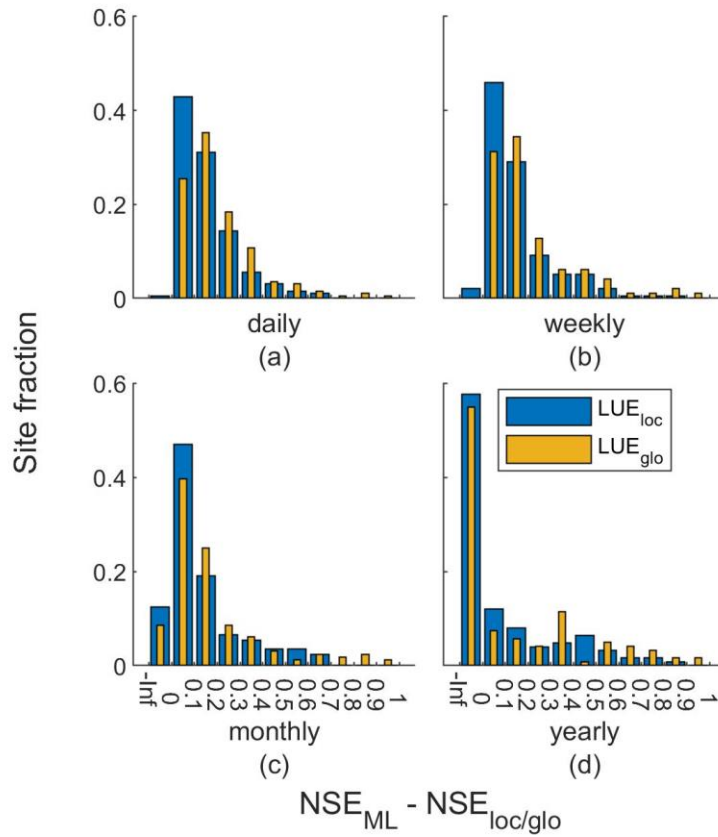
69
70 **Figure S 6. The model rank of all the LUE models based on the likelihood derived from approximate**
71 **Bayesian computation scheme, which can represent the goodness of a model across bootstrapped sites,**
72 **parameters and model fitness thresholds.** The yellow asterisk is the global best model selected according to
73 site-sampling method (model #1), which is the second-best model here. Blue asterisks are the published
74 models of which the likelihoods are all zero.

75



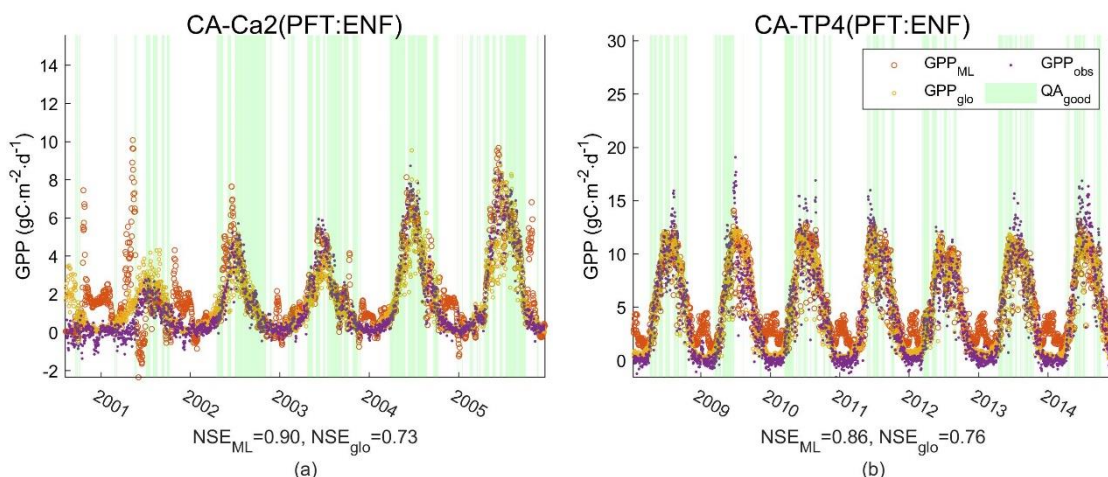
76

77 **Figure S 7. The time series GPP from EC sites (GPP_{obs}), GPP simulated using the global best model
78 (GPP_{glo}), the site-best models (GPP_{loc}) and the best machine learning model (GPP_{ML}) at a) CN-Ha2 (the
79 largest NSE), b) CA-Ca2 (the NSE median), c) DK-Ris (the NSE at the 25th percentile), and d) FR-Lq1
80 (the smallest NSE). The transparent green area represents the period with the good-quality forcing data and
81 GPP_{obs} (QA_{good}), the NSE_{loc} and NSE_{glo} are the NSE of GPP_{loc} against GPP_{obs} and GPP_{glo} against GPP_{obs} within
82 QA_{good} period at the daily scale, the plant functional types (PFT) of a-d were wetland (WET), evergreen
83 needleleaf forest (ENF), cropland (CRO) and grassland (GRA).**



84
85
86
87
88

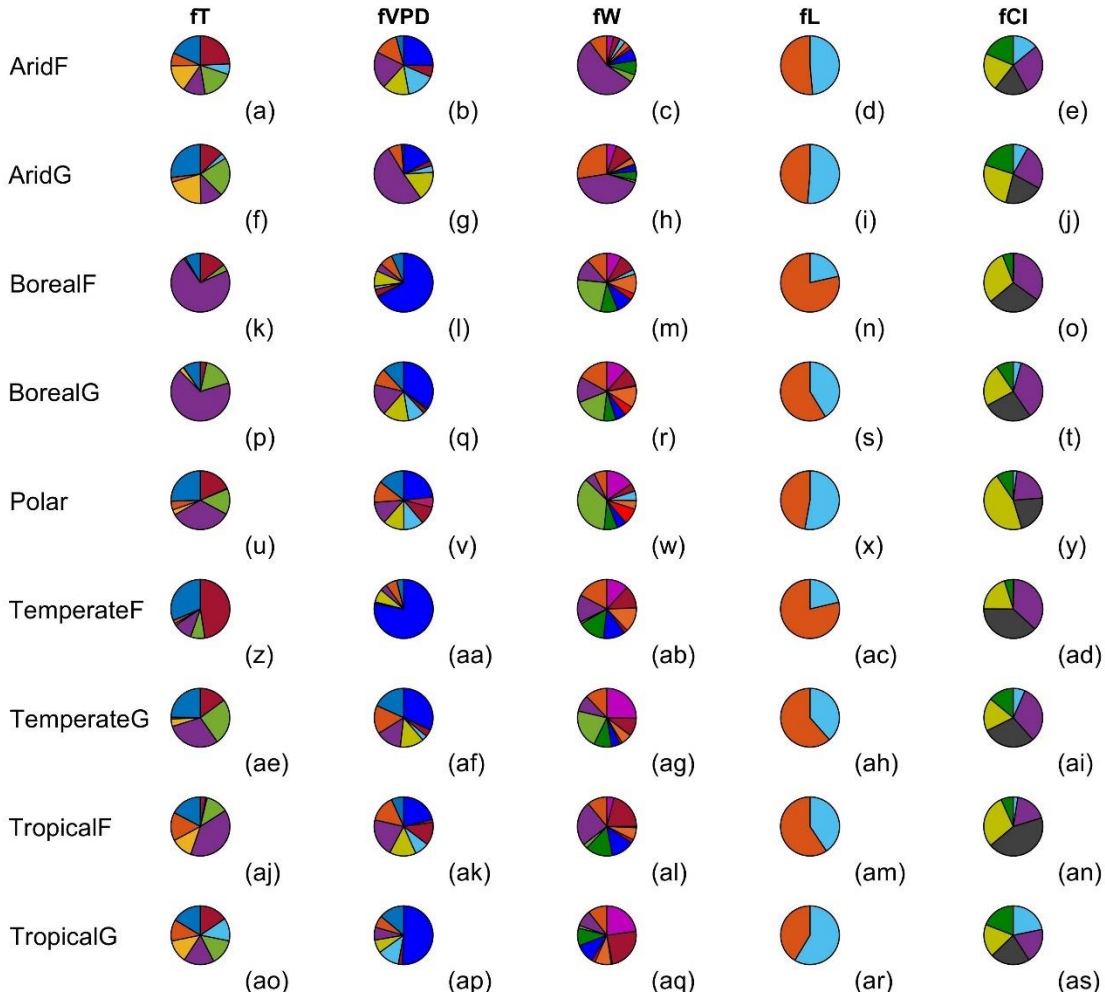
Figure S 8. Differences between NSE of the site-best machine learning models and site-best LUE models (LUE_{loc}) and differences between NSE of the site-best machine learning models and the global best LUE model (LUE_{glo}) at a daily scale. NSE_{ML} and NSE_{loc/glo} represent the NSE of the site-best machine learning models, and LUE_{loc} and LUE_{glo}.



89
90
91
92
93
94

Figure S 9. The time series GPP from EC sites (GPP_{obs}), GPP simulated using the global best model (GPP_{glo}), and the best machine learning model (GPP_{ML}) at a) CA-Ca2, b) CA-TP4: the transparent green area represents the period with the good-quality forcing data and GPP_{obs} (QA_{good}), the NSE_{ML} and NSE_{glo} are the NSE of GPP_{ML} against GPP_{obs} and GPP_{glo} against GPP_{obs} within QA_{good} period at the daily scale.

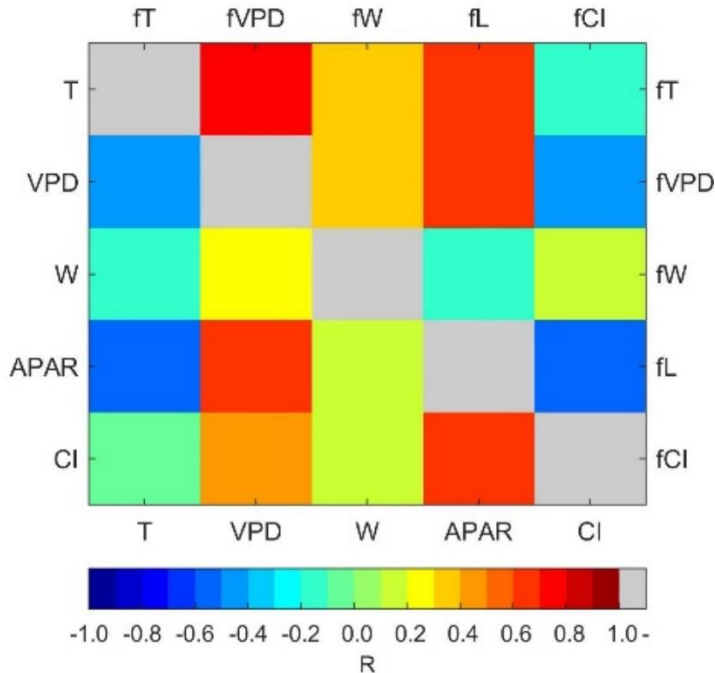
In the best 1% models



95

96

97 **Figure S 10. Likelihood of partial sensitivity functions in the best 1% models according to the average P₁**
98 **and P₂, for: arid forest (AridF), arid grassland (AridG), boreal forest (BorealF), boreal grassland**
99 **(BorealG), polar vegetation (Polar), temperate forest (TemperateF), temperate grassland (TemperateG),**
100 **tropical forest (TropicalF) and tropical grassland (TropicalG)**



101

102 **Figure S 11. Correlation matrix between environmental factors and partial sensitivity functions derived**
 103 **from the global best model.** The left and lower half matrix represent the average correlation coefficient (R)
 104 between temperature (T), vapor pressure deficit (VPD), soil water supply (W), absorbed photosynthetically
 105 active radiation (APAR) and cloudiness index (CI) of all sites. The right and upper half matrix represent the
 106 average R between the partial sensitivity functions of T (fT), VPD (fVPD), W (fW), light saturation (fL) and
 107 CI (fCI) of all sites. The gray area is empty. The red and blue colors represent high correlations between the
 108 variables (e.g., T and VPD, T and APAR, CI and APAR, fT and fVPD, fT and fL, fCI and fL).

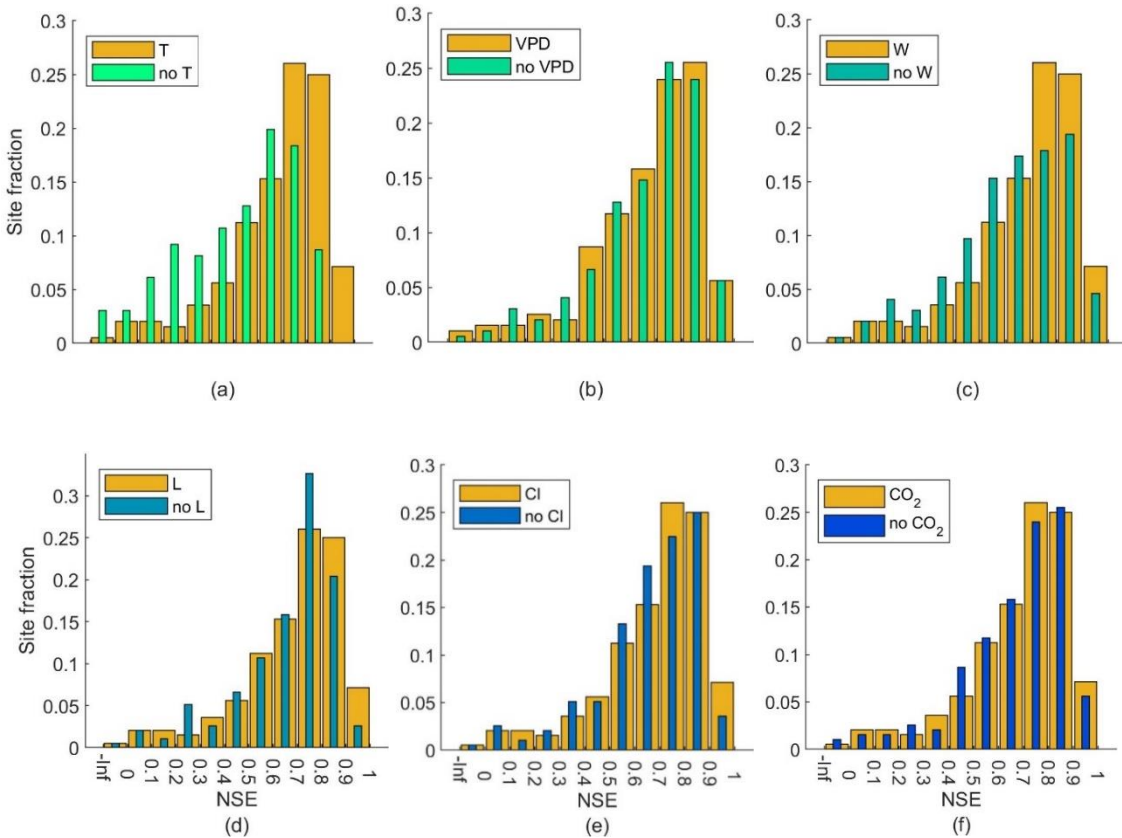


Figure S 12. The comparison between the global best model with full factors (the wide orange bar) and the best model ignoring T (narrow bar in a), VPD (narrow bar in b, here the wide bar represent the best model with only T, VPD, W, L and CI effects and without CO₂ effect), W (narrow bar in c), L (narrow bar in d), CI (narrow bar in e) and CO₂ (narrow bar in f) effect at the daily scale. The differences between the bars represent the reduced model efficiency due to ignoring the variability of a climatic factor.

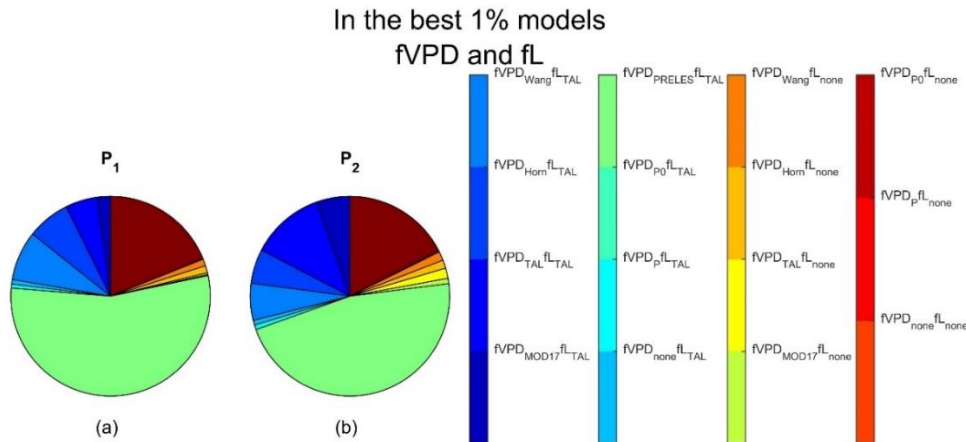
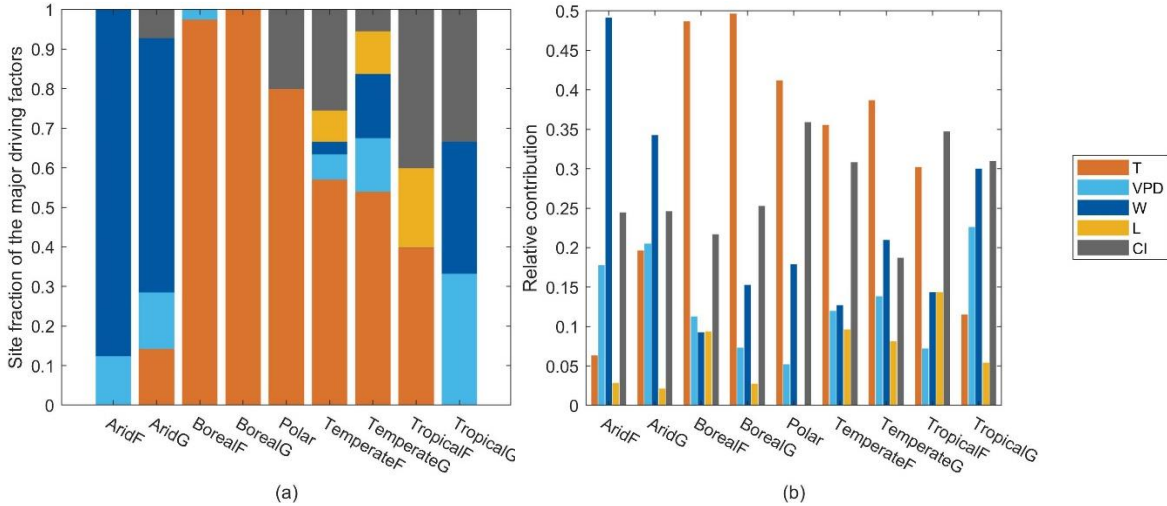
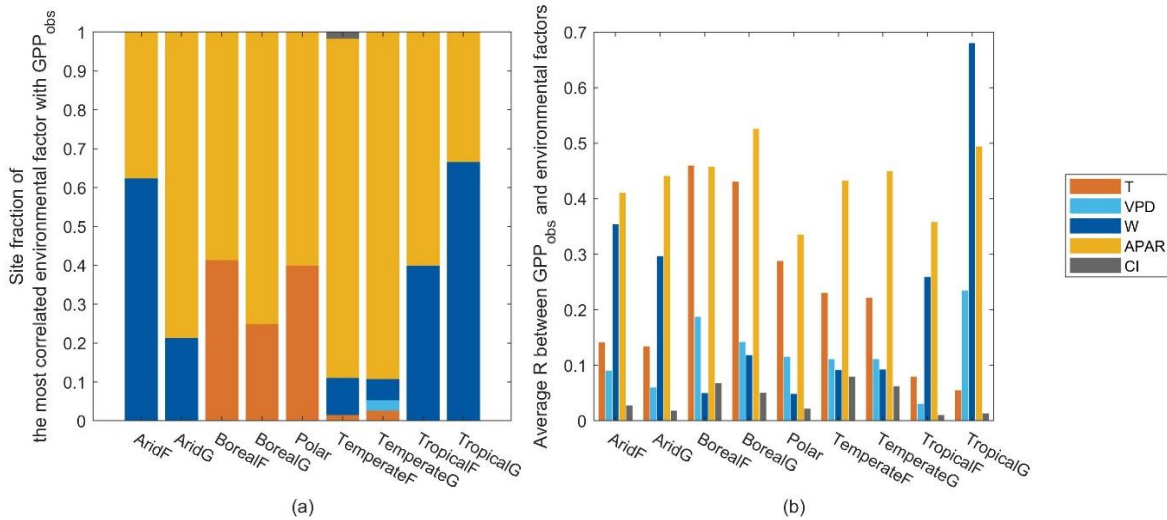


Figure S 13. Likelihood of different fVPD and fL combinations in the best 1% models

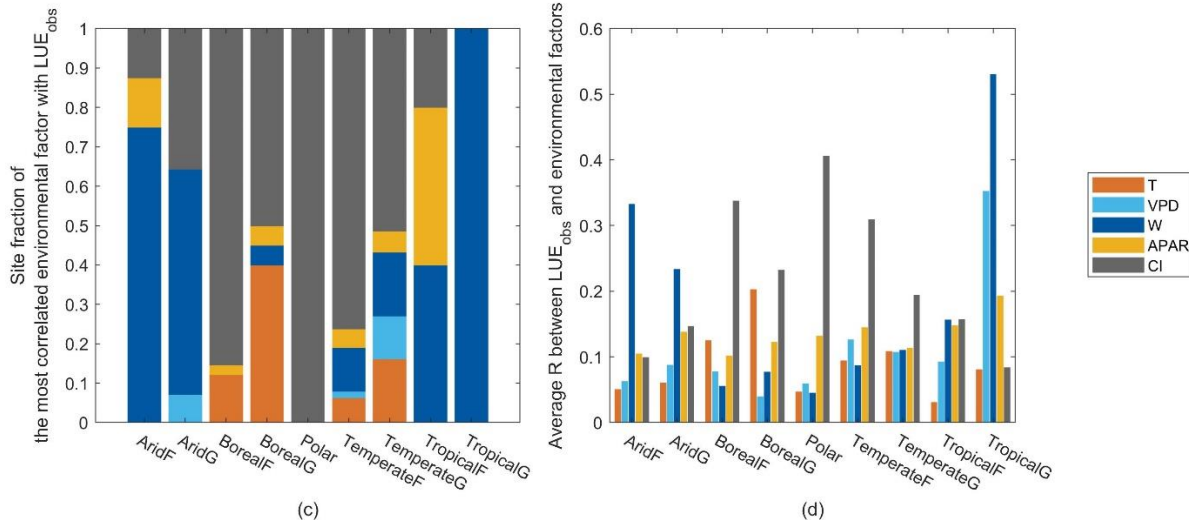


120

121 **Figure S 14. Environment sensitivities in the site-best models across different climate-vegetation types:**
122 **(a) Site fraction of the major driving factor and (b) relative contribution of each environmental factor.** T
123 (orange) is temperature, VPD (sky blue) is vapor pressure deficit, W (dark blue) is soil water supply, L(yellow)
124 is light saturation and CI (gray) is cloudiness index in both figures. ‘Major driving factor’ represents the
125 environmental factor that has the strongest effect on LUE at site-level. ‘Relative contribution’ is a measure of
126 the contribution of an environmental factor to the total limitation on LUE at site level and is averaged per
127 climate-vegetation type.

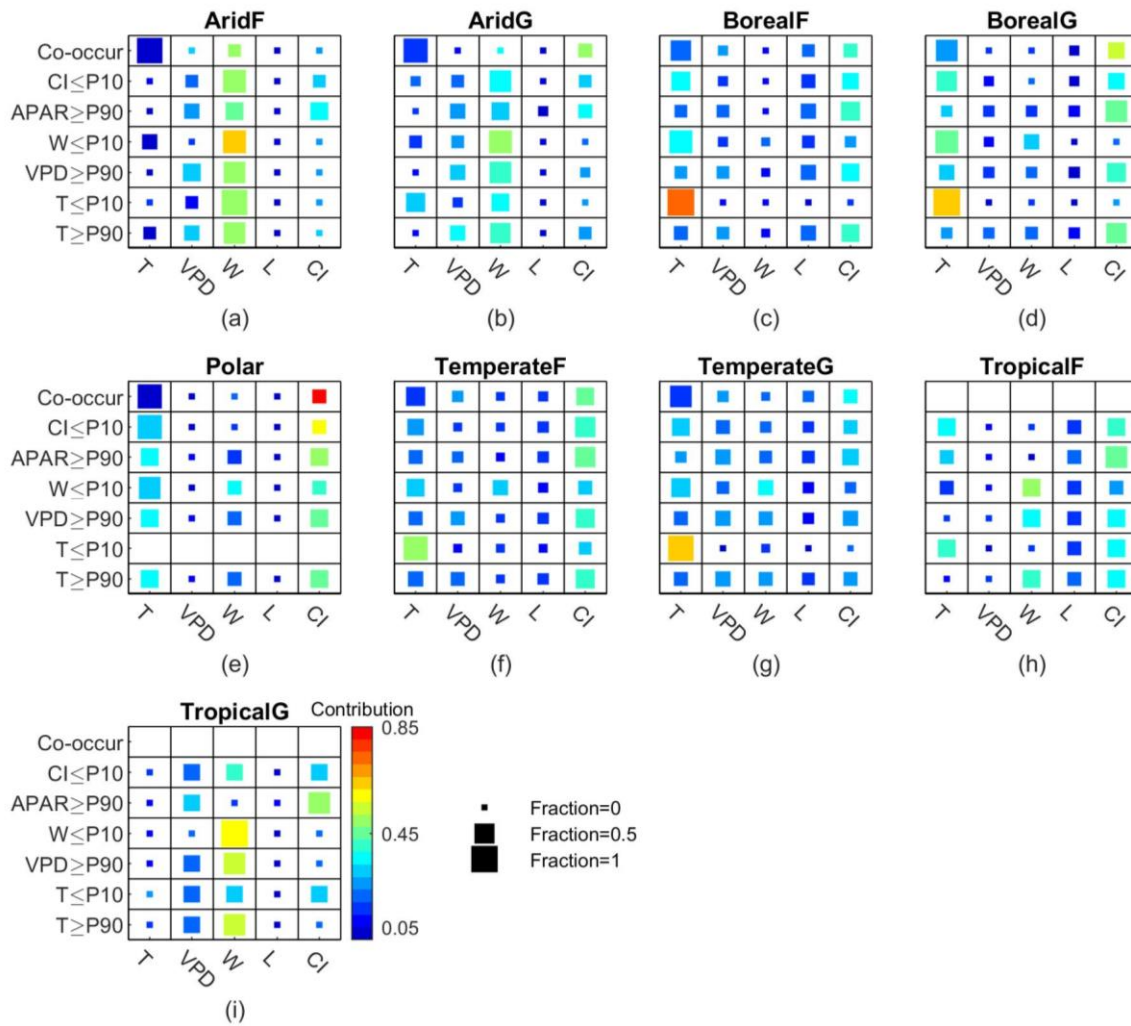


128



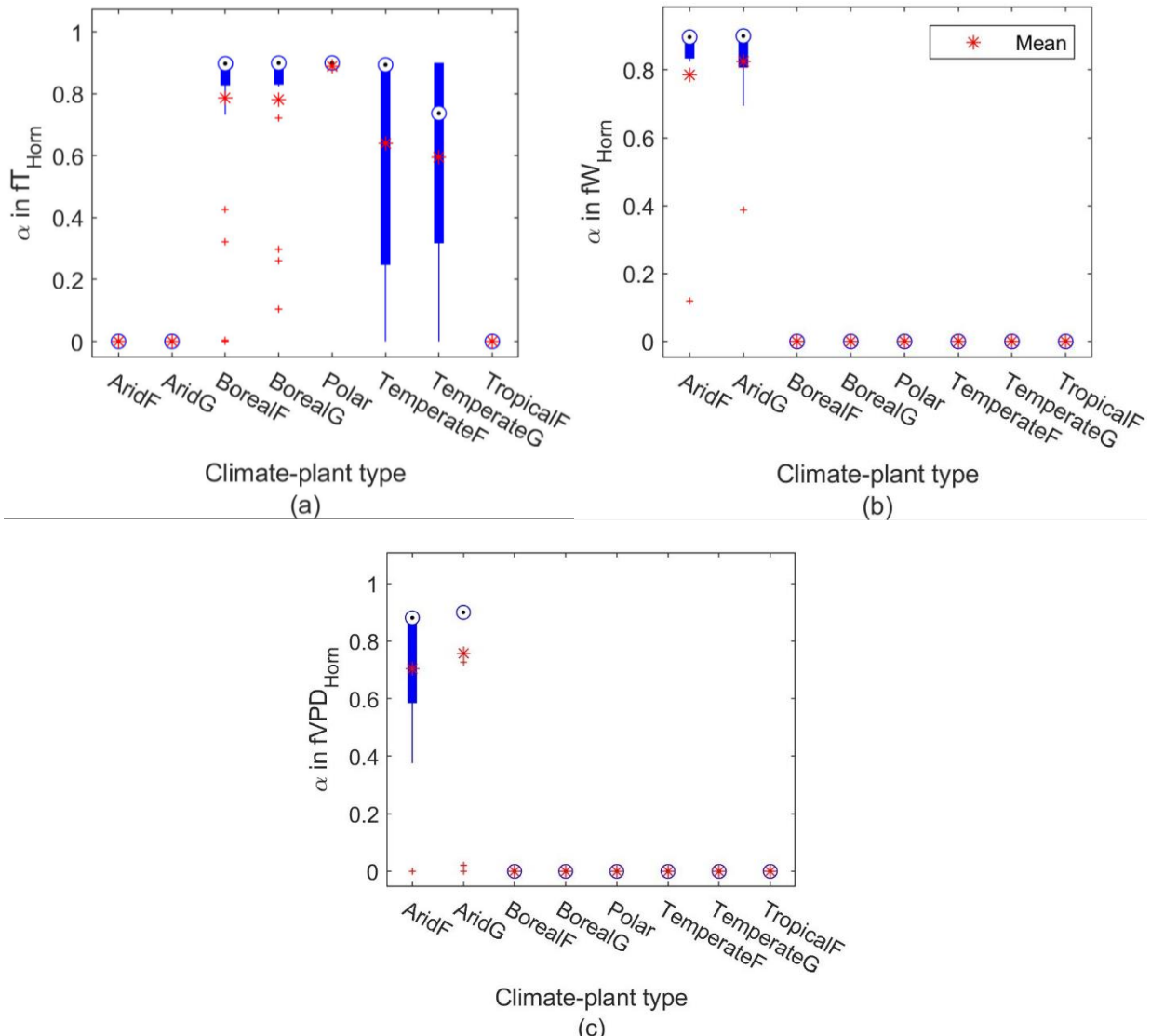
129

Figure S 15. Driving factors of different climate-vegetation types according to the observations: (a) Site fraction of the environmental factors with the maximum absolute correlation coefficient (R) with GPP_{obs} ; (b) average R between GPP_{obs} and environmental factors; (c) Site fraction of the environmental factor with the maximum absolute R between LUE_{obs} and environmental factors; (d) average R between LUE_{obs} and environmental factors



135

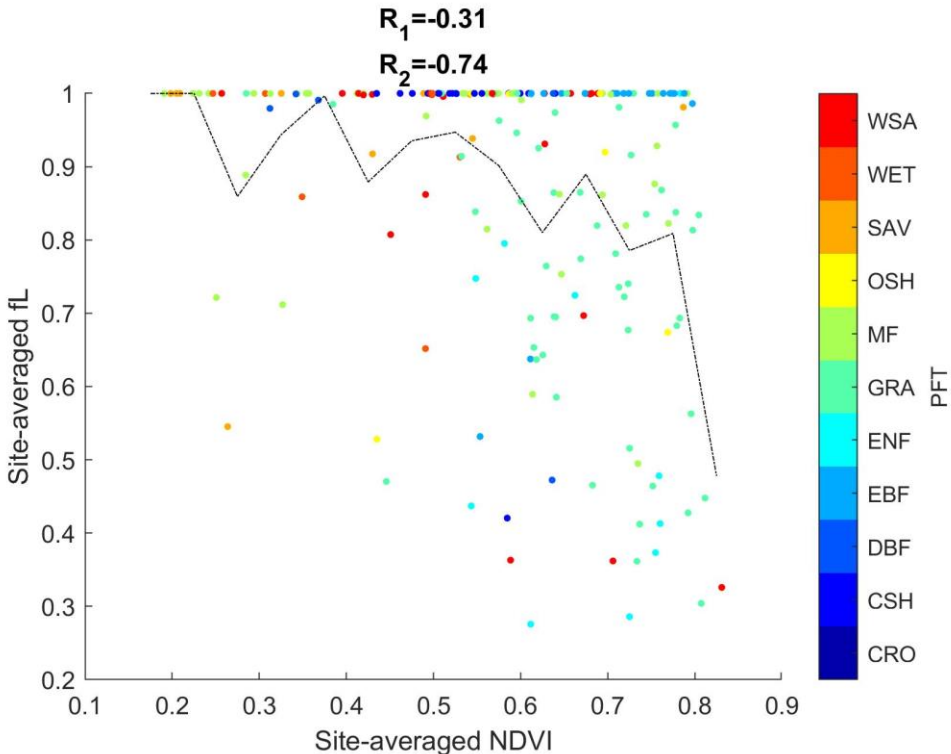
136 **Figure S 16. Environment sensitivities of LUE in the site-best models under extreme conditions across**
137 **different climate-vegetation types: site fraction of each ‘major driving factor’ (indicated by the size of the**
138 **squares) and ‘relative contribution’ of each environmental factor (indicated by the color of the squares).**
139 **X-axis represents the environmental factors: temperature (T), vapor pressure deficit (VPD), soil water supply**
140 **(W), light saturation (L), cloudiness (CI). ‘Co-occur’ represents the environmental condition at site level when**
141 **T≥90th percentile, VPD≥90th percentile, W≤10th percentile, APAR≥90th percentile, and CI≤10th percentile.**
142 **There are no ‘Co-occur’ points at tropical sites (h and i). CI≤P10, APAR≥P90, W≤P10, VPD≥P90, T≤P10 and**
143 **T≥P90 represent the environmental conditions that CI≤10th percentile (clear skies), APAR≥90th percentile**
144 **(intense light), W≤10th percentile (low soil water availability), VPD≥90th percentile (high atmospheric water**
145 **demand), T≤10th percentile (low temperature), and T≥90th percentile (high temperature), respectively. The**
146 **larger a square is, the more sites at which an environmental factor has the strongest effect on LUE. The more**
147 **bright (yellow and red color) a square is, the larger the relative contribution of an environmental factor to the**
148 **total limitation on LUE is.**



149

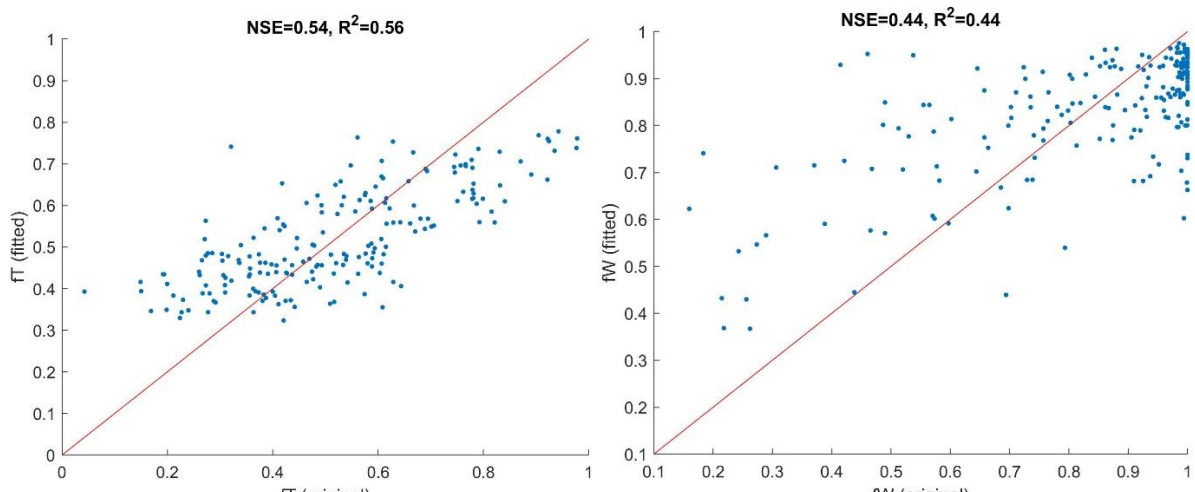
150

151 **Figure S 17. Distribution of values of the lag parameter (α) of fT_{Horn} (a) and fW_{Horn} (b) in the global best
152 model and α of fVPD_{Horn} (c) in another LUE model with the highest rank among the models with
153 fVPD_{Horn} (α represents the degree of the delayed response of LUE to the variations in temperature, soil water
154 supply or vapor pressure deficit; the blue box represents the interquartile range of α , the black target refers to
155 the median and the red asterisk is the mean; α close to 0.9 indicates an apparent delay process to the triggering
156 variable.)**



157

158 **Figure S 18. Scatters of site-averaged fL against site-averaged NDVI, colored by plant functional type**
 159 (**PFT**). The black line (-) is the trend between bin-averaged fL and NDVI (the bins are NDVI=0.2-0.25, 0.25-
 160 0.3, 0.3-0.35, 0.35-0.4, 0.4-0.45, 0.45-0.5, 0.5-0.55, 0.55-0.6, 0.6-0.65, 0.65-0.7, 0.7-0.75, 0.75-0.8, and 0.8-0.85).
 161 The correlation coefficient (R_1) between site-average fL and NDVI (i.e., the colorful scatters) is -0.31. The R
 162 between the bin-averaged fL and NDVI (i.e., the black line), R_2 , is -0.74.



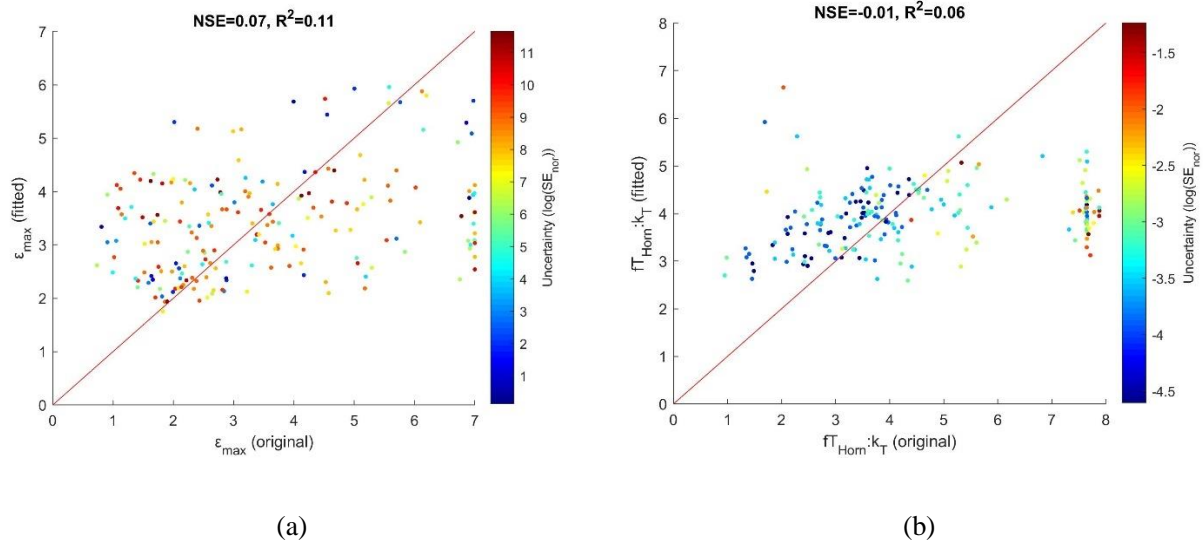
163

164

(a)

(b)

165 **Figure S 19. Fitted site-averaged fT and fW using site-specific properties based on random forest**
 166 **method against the original fT (a) and fW (b) of the global best calculated using calibrated parameters**



173 **Tables**

174

Table S 1. The names and partial sensitivity functions of published models

Model Name	fT	fVPD	fW	fL	fCI	Reference
CFlux	fT _{MOD17}	fVPD _{MOD17}	fW _{CFlux}	fL _{none}	fL _{CFlux}	(Turner et al., 2006)
Horn	fT _{Horn}	fVPD _{none}	fW _{Horn}	fL _{none}	fL _{none}	(Horn et al., 2011)
Horn ₁	fT _{Horn}	fVPD _{Horn}	fW _{none}	fL _{none}	fL _{none}	As above
MODIS	fT _{MOD17}	fVPD _{MOD17}	fW _{none}	fL _{none}	fL _{none}	(Running et al., 2004)
P	fT _P	fVPD _P	fW _P	fL _{none}	fL _{none}	(Stocker et al., 2020)
P ₀	fT _P	fVPD _{P0}	fW _P	fL _{none}	fL _{none}	As above
PRELES	fT _{TAL}	fVPD _{PRELES}	fW _{PRELES}	fL _{TAL}	fL _{none}	(Kalliokoski et al., 2018)
TAL	fT _{TAL}	fVPD _{TAL}	fW _{TAL}	fL _{TAL}	fL _{none}	(Mäkelä et al., 2008)
TAL ₁	fT _{TAL}	fVPD _{TAL}	fW _{TAL1}	fL _{TAL}	fL _{none}	As above
VPM	fT _{VPM}	fVPD _{none}	fW _{VPM}	fL _{none}	fL _{none}	(Xiao et al., 2004)
Wang	fT _{CASA}	fVPD _{Wang}	fW _{WAI}	fL _{none}	fL _{Wang}	(Wang et al., 2018)

175

Table S 2. Eddy covariance site list used in this study (PFT: plant functional type)

SiteID	Lat	Lon	Data start (year)	Data end (year)	PFT	Climate type	Elevation(m)	Reference
AR-SLu	-33.5	-66.5	2010	2011	MF	BSh	506 ^{*e}	(Ulke et al., 2015)
AT-Neu	47.1	11.3	2002	2012	GRA	Dfc	970	(Wohlfahrt et al., 2008)
AU-ASM	-22.3	133.3	2010	2014	ENF	BWh	606 ^{*b}	(Cleverly et al., 2013)
AU-Cpr	-34.0	140.6	2010	2014	SAV	BSk	62 ^{*e}	(Bloomfield et al., 2018; Meyer et al., 2015)
AU-Cum	-33.6	150.7	2012	2014	EBF	Cfa	20	(Renchon et al., 2018)
AU-DaP	-14.1	131.3	2009	2013	GRA	Aw	71 ^{*e}	(Hutley et al., 2011)

AU-DaS	-14.2	131.4	2010	2014	SAV	Aw	110	(Hutley et al., 2011)
AU-Dry	-15.3	132.4	2008	2014	SAV	Aw	175	(Hutley et al., 2011)
AU-Emr	-23.9	148.5	2011	2013	GRA	BSh	170	(Schroder, 2014)
AU-Gin	-31.4	115.7	2013	2014	WSA	Csa	51	(Beringer et al., 2016)
AU-GWW	-30.2	120.7	2011	2014	SAV	BSh	450	(Beringer et al., 2016)
AU-How	-12.5	131.2	2001	2014	WSA	Aw	64	(Beringer et al., 2003)
AU-RDF	-14.6	132.5	2011	2013	WSA	Aw	188 ^{*e}	(Bristow et al., 2016)
AU-Rig	-36.7	145.6	2011	2014	GRA	Cfa	152	(Beringer et al., 2016)
AU-Stp	-17.2	133.4	2008	2014	GRA	BSh	250 ^{*b}	(Hutley et al., 2011)
AU-TTE	-22.3	133.6	2012	2014	OSH	BWh	553	(Cleverly et al., 2016)
AU-Tum	-35.7	148.2	2001	2014	EBF	Cfb	1200	(Leuning et al., 2005)
AU-Wom	-37.4	144.1	2010	2014	EBF	Cfb	705	(Griebel et al., 2016)
AU-Ync	-35.0	146.3	2012	2014	GRA	BSk	126 ^{*e}	(Yee et al., 2015)
BE-Bra	51.3	4.5	2000	2014	MF	Cfb	16 ^{*a}	(Carrara et al., 2004)
BE-Lon	50.6	4.8	2004	2014	CRO	Cfb	167	(Aubinet et al., 2009)
BE-Vie	50.3	6.0	2000	2014	MF	Cfb	450 ^{*a}	As above
BR-Ban	-9.8	-50.2	2003	2006	EBF	Aw	120	(Da Rocha et al., 2009)
BR-Sp1	-21.6	-47.7	2001	2002	WSA	Aw	690	As above
BW-Ma1	-19.9	23.6	2000	2001	WSA	BSh	950	(Veenendaal et al., 2004)
CA-Ca1	49.9	-125.3	2000	2005	ENF	Cfb	300	(Humphreys et al., 2006)
CA-Ca2	49.9	-125.3	2000	2005	ENF	Csb	300	As above
CA-Ca3	49.5	-124.9	2001	2005	ENF	Csb	300	As above
CA-Gro	48.2	-82.2	2003	2014	MF	Dfb	340	(Pejam et al., 2006)
CA-Let	49.7	-112.9	2000	2005	GRA	BSk	960	(Flanagan et al., 2002)
CA-Mer	45.4	-75.5	2000	2005	WET	Dfb	70	(Lafleur et al., 2003)

CA-NS2	55.9	-98.5	2002	2005	ENF	Dfc	260	(Beringer et al., 2011)
CA-NS3	55.9	-98.4	2001	2005	ENF	Dfc	260	As above
CA-NS4	55.9	-98.4	2002	2005	ENF	Dfc	260	As above
CA-NS5	55.9	-98.5	2002	2005	ENF	Dfc	260	As above
CA-NS6	55.9	-99.0	2001	2005	OSH	Dfc	244	As above
CA-NS7	56.6	-100.0	2002	2005	OSH	Dfc	297	As above
CA-Oas	53.6	-106.2	2000	2010	DBF	Dfc	530	(Black et al., 1996)
CA-Obs	54.0	-105.1	2000	2010	ENF	Dfc	628.94	(Jarvis et al., 1997)
CA-Ojp	53.9	-104.7	2000	2005	ENF	Dfb	579	(Baldocchi et al., 1997)
CA-Qcu	49.3	-74.0	2001	2006	ENF	Dfb	392.3	(Giasson et al., 2006)
CA-Qfo	49.7	-74.3	2004	2010	ENF	Dfc	382	(Bergeron et al., 2007)
CA-SF1	54.5	-105.8	2003	2006	ENF	Dfc	536	(Mkhabela et al., 2009)
CA-SF2	54.3	-105.9	2001	2005	ENF	Dfc	520	As above
CA-SF3	54.1	-106.0	2001	2005	OSH	Dfc	540	As above
CA-SJ1	53.9	-104.7	2001	2005	ENF	Dfb	580	(Howard et al., 2004)
CA-SJ2	53.9	-104.7	2003	2005	ENF	Dfc	580	(Coursolle et al., 2012)
CA-TP1	42.7	-80.6	2008	2014	ENF	Dfb	265	(Peichl et al., 2007)
CA-TP3	42.7	-80.4	2008	2014	ENF	Dfb	184	As above
CA-TP4	42.7	-80.4	2008	2014	ENF	Dfb	184	(Arain et al., 2005)
CA-TPD	42.6	-80.6	2012	2014	DBF	Dfb	260	As above
CA-WP1	55.0	-112.5	2003	2005	WET	Dfc	540	(Syed et al., 2006)
CH-Cha	47.2	8.4	2005	2014	GRA	Cfb	393	(Merbold, Lutz et al., 2014)
CH-Dav	46.8	9.9	2000	2014	ENF	ET	1639	(Wolf et al., 2013; Zielis et al., 2014)
CH-Fru	47.1	8.5	2005	2014	GRA	Cfb	982	(Imer et al., 2013)
CH-Oe1	47.3	7.7	2002	2008	GRA	Cfb	450	(Ammann et al., 2009)
CN-Cha	42.4	128.1	2003	2005	MF	Dwb	738	(Zhang et al., 2006)

CN-Cng	44.6	123.5	2007	2010	GRA	BSk	171 ^{*d}	(Pastorello et al., 2020)
CN-Dan	30.5	91.1	2004	2005	GRA	Dwc	4286	(Shi et al., 2006)
CN-Du2	42.1	116.3	2006	2008	GRA	Dwb	1350 ^{*b}	(Chen et al., 2009)
CN-Ha2	37.6	101.3	2003	2005	WET	Dwc	3357	(Pastorello et al., 2020)
CN-Xfs	44.1	116.3	2004	2006	GRA	BSk	1250	(Chen et al., 2009)
CZ-BK1	49.5	18.5	2004	2014	ENF	Dfb	908 ^{*a}	(Krupková et al., 2017)
CZ-BK2	49.5	18.5	2009	2012	GRA	Dfb	855	(Acosta et al., 2013)
CZ-wet	49.0	14.8	2007	2014	WET	Cfb	426	(Dušek et al., 2012)
DE-Geb	51.1	10.9	2001	2014	CRO	Cfb	161.5	(Anthoni et al., 2004b)
DE-Gri	51.0	13.5	2004	2014	GRA	Cfb	385	(Prescher et al., 2010)
DE-Hai	51.1	10.5	2000	2009	DBF	Cfb	430 ^{*a}	(Knöhl et al., 2003)
DE-Har	47.9	7.6	2005	2006	ENF	Cfb	201	(Pastorello et al., 2020)
DE-Kli	50.9	13.5	2004	2014	CRO	Cfb	478	(Prescher et al., 2010)
DE-Lnf	51.3	10.4	2002	2012	DBF	Cfb	451	(Anthoni et al., 2004a)
DE-Meh	51.3	10.7	2003	2006	MF	Cfb	293 ^{*a}	(DON et al., 2009)
DE-Obe	50.8	13.7	2008	2014	ENF	Cfb	734	(Pastorello et al., 2020)
DE-SfN	47.8	11.3	2013	2014	WET	Cfb	590	(Hommeltenberg et al., 2014)
DE-Tha	51.0	13.6	2000	2014	ENF	Cfb	380 ^{*a}	(Bernhofer et al., 2003)
DE-Wet	50.5	11.5	2002	2006	ENF	Cfb	785 ^{*a}	(Rebmann et al., 2010)
DK-Ris	55.5	12.1	2004	2005	CRO	Cfb	10	(Pastorello et al., 2020)
DK-Sor	55.5	11.6	2000	2014	DBF	Cfb	40 ^{*a}	(Pilegaard et al., 2020)

ES-Amo	36.8	-2.3	2000	2014	OSH	BSh	58	(López-Ballesteros et al., 2017)
ES-ES1	39.4	-0.3	2007	2012	ENF	Csa	5 ^{*a}	(Sanz M J, 2004)
ES-ES2	39.3	-0.3	2000	2006	CRO	Csa	10	As above
ES-LgS	37.1	-3.0	2004	2006	OSH	Csb	2267	(Reverter et al., 2010)
ES-LJu	36.9	-2.8	2005	2011	OSH	Csa	1600	(Serrano-Ortiz et al., 2009)
ES-LMa	39.9	-5.8	2004	2006	SAV	Csa	258 ^{*a}	(Perez-Priego et al., 2017)
ES-VDA	42.2	1.5	2007	2009	GRA	Cfb	1765 ^{*a}	(Pastorello et al., 2020)
FI-Hyy	61.9	24.3	2004	2006	ENF	Dfc	181 ^{*a}	(Suni et al., 2003)
FI-Kaa	69.1	27.3	2000	2014	WET	Dfc	155	(AURELA, MIKA et al., 2007)
FI-Let	60.6	24.0	2000	2006	ENF	Dfb	111	(Koskinen et al., 2014)
FI-Lom	68.0	24.2	2009	2012	WET	Dfc	269 ^{*a}	(Aurela, M. et al., 2015)
FI-Sod	67.4	26.6	2007	2009	ENF	Dfc	180 ^{*a}	(Thum et al., 2007)
FR-Fon	48.5	2.8	2008	2014	DBF	Cfb	92 ^{*a}	(Michelot et al., 2011)
FR-Gri	48.8	2.0	2005	2013	CRO	Cfb	125	(Loubet et al., 2011)
FR-Hes	48.7	7.1	2004	2014	DBF	Cfb	300 ^{*a}	(Granier et al., 2000)
FR-LBr	44.7	-0.8	2000	2006	ENF	Cfb	61 ^{*a}	(Borbigier et al., 2001)
FR-Lq1	45.6	2.7	2000	2008	GRA	Cfb	1040	(Pastorello et al., 2020)
FR-Lq2	45.6	2.7	2004	2006	GRA	Cfb	1040	(Pastorello et al., 2020)
FR-Pue	43.7	3.6	2004	2006	EBF	Csa	270 ^{*a}	(Rambal et al., 2004)
GL-ZaH	74.5	-20.6	2000	2014	GRA	ET	48	(Lund et al., 2012)
HU-Bug	46.7	19.6	2002	2006	GRA	Cfb	111 ^{*a}	(Pastorello et al., 2020)

IL-Yat	31.3	35.1	2001	2006	ENF	Csa	650	(Tatarinov et al., 2016)
IT-Amp	41.9	13.6	2002	2006	GRA	Cfb	884 ^{*a}	(Papale et al., 2015)
IT-BCi	40.5	15.0	2004	2012	CRO	Csa	20	(Vitale et al., 2016)
IT-CA1	42.4	12.0	2011	2014	DBF	Csa	200	(Sabbatini et al., 2016)
IT-CA2	42.4	12.0	2011	2014	CRO	Csa	200	(Sabbatini et al., 2016)
IT-CA3	42.4	12.0	2011	2014	DBF	Csa	197	(Sabbatini et al., 2016)
IT-Col	41.9	13.6	2004	2014	DBF	Cfb	1560 ^{*a}	(VALENTINI et al., 1996)
IT-Cpz	41.7	12.4	2000	2008	EBF	Csa	68	(Tirone et al., 2003)
IT-Isp	45.8	8.6	2013	2014	DBF	Cfa	210	(Ferréa et al., 2012)
IT-Lav	46.0	11.3	2004	2014	ENF	Cfb	1353	(Marcolla, B. et al., 2003)
IT-Lec	43.3	11.3	2005	2006	EBF	Csa	314	(Pastorello et al., 2020)
IT-MBo	46.0	11.1	2003	2013	GRA	Dfb	1550 ^{*a}	(Marcolla, Barbara et al., 2005)
IT-Noe	40.6	8.2	2004	2014	CSH	Csa	25	(Papale et al., 2015)
IT-Non	44.7	11.1	2001	2006	MF	Cfa	25 ^{*c}	(Nardino, 2002)
IT-PT1	45.2	9.1	2002	2004	DBF	Cfa	60	(Migliavacca et al., 2009)
IT-Ren	46.6	11.4	2002	2013	ENF	Dfc	1730 ^{*a}	(Marcolla, Barbara et al., 2005)
IT-Ro1	42.4	11.9	2000	2008	DBF	Csa	235	(Rey et al., 2002)
IT-Ro2	42.4	11.9	2002	2012	DBF	Csa	224 ^{*a}	(TEDESCHI et al., 2006)
IT-SR2	43.7	10.3	2013	2014	ENF	Csa	4	(Pastorello et al., 2020)
IT-SRo	43.7	10.3	2000	2012	ENF	Csa	4 ^{*a}	(Chiesi et al., 2005)
IT-Tor	45.8	7.6	2008	2012	GRA	ET	2160	(Galvagno et al., 2013)
NL-Ca1	52.0	4.9	2003	2006	GRA	Cfb	0.7	(Jacobs et al., 2007)

NL-Loo	52.2	5.7	2000	2014	ENF	Cfb	25 ^{*a}	(Dolman et al., 2002)
PT-Cor	39.1	-8.3	2010	2017	EBF	Csa	170 ^{*c}	(Pastorello et al., 2020)
PT-Esp	38.6	-8.6	2002	2006	EBF	Csa	95 ^{*a}	(Rodrigues et al., 2011)
PT-Mi1	38.5	-8.0	2003	2005	EBF	Csa	264 ^{*a}	(Pereira et al., 2007)
PT-Mi2	38.5	-8.0	2004	2006	GRA	Csa	190	(Pereira et al., 2007)
RU-Fyo	56.5	32.9	2002	2014	ENF	Dfb	265 ^{*a}	(Kurbatova et al., 2008)
RU-Ha1	54.7	90.0	2002	2004	GRA	Dfb	446	(Belelli Marchesini et al., 2007)
RU-Zot	60.8	89.4	2002	2004	ENF	Dfc	90	(Arneth et al., 2002)
SD-Dem	13.3	30.5	2007	2009	SAV	BWh	500	(Ardö et al., 2008)
SE-Deg	64.2	19.6	2001	2005	WET	Dfc	270	(Sagerfors et al., 2008)
SE-Fla	64.1	19.5	2000	2002	ENF	Dfc	226 ^{*c}	(Valentini et al., 2000)
US-AR1	36.4	-99.4	2009	2012	GRA	Cfa	611	(Billesbach D, 2016)
US-AR2	36.6	-99.6	2009	2012	GRA	Cfa	646	(Billesbach D, 2016)
US-ARb	35.6	-98.0	2003	2012	GRA	Cfa	424	(Pastorello et al., 2020)
US-ARc	35.6	-98.0	2005	2006	GRA	Cfa	424	(Pastorello et al., 2020)
US-ARM	36.6	-97.5	2005	2006	CRO	Cfa	314	(Pastorello et al., 2020)
US-Atq	70.5	-157.4	2003	2008	WET	ET	15	(Pastorello et al., 2020)
US-Aud	31.6	-110.5	2002	2006	GRA	BSk	1469	(Pastorello et al., 2020)
US-Bar	44.1	-71.3	2004	2005	DBF	Dfb	272	(Ouimette et al., 2018)
US-Bkg	44.4	-96.8	2004	2006	GRA	Dfa	510	(Gilmanov et al., 2005)

US-Blo	38.9	-120.6	2000	2007	ENF	Csb	1315	(Goldstein et al., 2000)
US-Bo1	40.0	-88.3	2000	2007	CRO	Cfa	219	(Pastorello et al., 2020)
US-Bo2	40.0	-88.3	2004	2006	CRO	Cfa	219	(Pastorello et al., 2020)
US-Cop	38.1	-109.4	2011	2013	GRA	BSk	1520	(D., 2016)
US-CRT	41.6	-83.4	2001	2007	CRO	Dfa	180	(Pastorello et al., 2020)
US-Dk1	36.0	-79.1	2001	2005	GRA	Cfa	168	(Pastorello et al., 2020)
US-Dk3	36.0	-79.1	2001	2005	ENF	Cfa	163	(Pastorello et al., 2020)
US-Fmf	35.1	-111.7	2000	2006	ENF	Csb	2160	(Pastorello et al., 2020)
US-FPe	48.3	-105.1	2004	2006	GRA	BSk	634	(Pastorello et al., 2020)
US-FR2	30.0	-98.0	2005	2006	WSA	Cfa	271.9	(Heinsch et al., 2004)
US-Goo	34.3	-89.9	2002	2006	GRA	Cfa	87	(T., 2016)
US-Ha1	42.5	-72.2	2000	2012	DBF	Dfb	340	(Urbanski et al., 2007)
US-Ho1	45.2	-68.7	2000	2004	ENF	Dfb	60	(Hollinger et al., 1999)
US-IB1	41.9	-88.2	2005	2007	CRO	Dfa	226.5	(Pastorello et al., 2020)
US-IB2	41.8	-88.2	2004	2011	GRA	Dfa	226.5	(Pastorello et al., 2020)
US-Ivo	68.5	-155.8	2004	2007	WET	ET	568	(Epstein et al., 2004)
US-KS2	28.6	-80.7	2003	2006	CSH	Cfa	3	(Powell et al., 2006)
US-Los	46.1	-90.0	2000	2014	WET	Dfb	480	(Sulman et al., 2009)
US-Me2	44.5	-121.6	2000	2014	ENF	Csb	1253	(Kwon et al., 2018; Thomas et al., 2009)

US-Me3	44.3	-121.6	2004	2006	ENF	Csb	1005	(Vickers et al., 2012)
US-Me5	44.4	-121.6	2002	2014	ENF	Csb	1188	(Law et al., 2001; Williams et al., 2001)
US-Me6	44.3	-121.6	2004	2009	ENF	Csb	998	(Ruehr et al., 2014)
US-MMS	39.3	-86.4	2000	2002	DBF	Cfa	275	(Roman et al., 2015)
US-MOz	38.7	-92.2	2010	2014	DBF	Cfa	219.4	(Gu et al., 2016)
US-Myb	38.1	-121.8	2011	2014	WET	Csa	-1	(Pastorello et al., 2020)
US-NC1	35.8	-76.7	2005	2006	OSH	Cfa	5	(Noormets et al., 2012)
US-NC2	35.8	-76.7	2005	2006	ENF	Cfa	5	(Pastorello et al., 2020)
US-Ne1	41.2	-96.5	2000	2014	CRO	Dfa	361	(Pastorello et al., 2020)
US-Ne2	41.2	-96.5	2001	2013	CRO	Dfa	362	(Pastorello et al., 2020)
US-Ne3	41.2	-96.4	2001	2013	CRO	Dfa	363	(Pastorello et al., 2020)
US-NR1	40.0	-105.6	2001	2013	ENF	Dfc	3050	(Monson et al., 2002)
US-Oho	41.6	-83.8	2004	2013	DBF	Dfa	230	(DeForest et al., 2006)
US-Prr	65.1	-147.5	2011	2014	ENF	Dfc	210	(Ikawa et al., 2015; Nakai et al., 2013)
US-SO2	33.4	-116.6	2004	2006	CSH	Csb	1394	(Lipson et al., 2005)
US-SO3	33.4	-116.6	2001	2006	CSH	Csb	1429	(Lipson et al., 2005)
US-SO4	33.4	-116.6	2004	2006	CSH	Csb	1429	(Lipson et al., 2005)
US-SP2	29.8	-82.2	2000	2004	ENF	Cfa	50	(Clark et al., 1999)
US-SP3	29.8	-82.2	2000	2004	ENF	Cfa	50	(Clark et al., 1999)
US-SRC	31.9	-110.8	2008	2014	OSH	BSh	991	(Pastorello et al., 2020)

US-SRG	31.8	-110.8	2008	2014	GRA	Csa	1291	(Scott et al., 2015)
US-SRM	31.8	-110.9	2004	2014	WSA	BSk	1120	(Scott et al., 2009)
US-Syv	46.2	-89.4	2001	2014	MF	Dfb	540	(Desai et al., 2005)
US-Ton	38.4	-121.0	2001	2014	WSA	Csa	177	(Ma et al., 2016)
US-Twt	38.1	-121.7	2009	2014	CRO	Csa	-7	(Pastorello et al., 2020)
US-UMB	45.6	-84.7	2000	2014	DBF	Dfb	234	(Gough et al., 2008)
US-Var	38.4	-121.0	2000	2014	GRA	Csa	129	(Ma et al., 2011)
US-WCr	45.8	-90.1	2000	2014	DBF	Dfb	520	(Cook et al., 2004)
US-Whs	31.7	-110.1	2011	2013	OSH	BSk	1370	(Pastorello et al., 2020)
US-Wi4	46.7	-91.2	2007	2014	ENF	Dfb	352	(Noormets et al., 2007)
US-Wi9	46.6	-91.1	2002	2005	ENF	Dfb	350	(Noormets et al., 2007)
US-Wkg	31.7	-109.9	2004	2005	GRA	BSk	1531	(Scott, 2010)
US-WPT	41.5	-83.0	2004	2014	WET	Cfa	175	(Pastorello et al., 2020)
US-Wrc	45.8	-122.0	2000	2006	ENF	Csb	371	(Wharton et al., 2012)
ZA-Kru	-25.0	31.5	2000	2012	SAV	BSh	359	(Archibald et al., 2009)
ZM-Mon	-15.4	23.3	2007	2009	WSA	Aw	1053	(Merbold, L. et al., 2009)

*a: collected from (Flechard et al., 2020).

*b: collected from (Hao et al., 2019).

*c: collected from (Tang, B. et al., 2018).

*d: collected from (Tang, X. et al., 2020).

*e: extracted from google earth.

Other elevation data were collected from <https://fluxnet.org/>, <http://www.europe-fluxdata.eu/>, <http://www.ozflux.org.au/>, <https://ameriflux.lbl.gov/>, <http://www.asiaflux.net/>, <http://www.chinaflux.org/>, and ancillary information of LaThuile dataset (<https://fluxnet.org/data/la-thuile-dataset/>).

177 **Table S 3. Model calibration experiments** (ϵ_{\max} and parameters of fX are LUE model parameters, AWC
 178 and are WAI parameters, the equations of cost function cf1, cf2 and cf3 are shown in the equation 12-14 in
 179 the main manuscript, ET and PET denote evapotranspiration and potential evapotranspiration,
 180 respectively)

Name	ϵ_{\max} and parameters of fX	AWC and θ	Cost function
Full	Optimized	Optimized	$cf1 + cf2 + cf3$
Sup	Optimized	Optimized	$cf1 + cf2 + cf3$, when $ET < PET$; 0, when $ET = PET$
Fix	Optimized	Fixed, AWC=150mm and $\theta=0.05$	$cf1 + cf3$
SupFix	Optimized	Fixed, AWC=150mm and $\theta=0.05$	$cf1 + cf3$, when $ET < PET$; 0, when $ET = PET$
IDP	Optimized	Optimize individually	$cf2$
SupIDP	Optimized	Optimize individually	$cf2$, when $ET < PET$; 0, when $ET = PET$

181 **Table S 4. Parameters initials and Ranges**

fX	Paramete r	Initial	Range	fX	Paramete r	Initial	Range
fT_{CASA}	ϵ_{max}	1	[0.01,7]	$fVPD_P$	c^*	0.41	[0.31,0.51]
	T_{opt}	25	[20,35]	$fVPD_P$	B	146	[118.4,291.6]
	T_a	0.2	[0.001,1]	$fVPD_{TAL}$	K	-0.005	[-1,-0.001]
	T_b	0.3	[0.001,1]	$fVPD_{Wan}$	D_θ	15	[1,500]
fT_{Horn}	T_{opt}	10	[5,35]	fW_{CFlux}	WHC_{max}	0.8	[0.1,1]
	k_T	2	[1,20]	fW_{CFlux}	WHC_{min}	0.5	[0.01,0.9]
	α	0.29	[0,0.9]	fW_{Horn}	W_I	0.4	[0.01,0.99]
fT_{MOD17}	$TMIN_{max}$	25	[5,30]	fW_{Horn}	k_w	-10	[-30,-5]
	$TMIN_{min}$	15	[-25,25]	fW_P	A	0.29	[0,0.9]
	A	0.352	[0,1]		Q	-1	[-20,-0.5]
fT_P	B	0.022	[0,1]	fW_P	θ^*	0.6	[0.1,1]
	C	0.0003	[0,0.01]	fW_{PRELES}	ρ	0.44897	[0.1,1]
	S_{max}	4	[0,0.01]			5	
fT_{TAL}	X_θ	15	[5,35]	fW_{TAL}	α	1.062	[0.1,1.3]
	T	-10	[-22,-8]	fW_{TAL}	v	11.27	[0.1,20]
	T_{opt}	13.75	[1,60]	fW_{TAL1}	α	15	[1,30]
fT_{VPM}	T_{max}	0.5	[0,1]	fW_{TAL1}	v	2	[1,20]
	T_{min}	30	[15,40]	fW_{VPM}	$LSWI_{max}$	0.41	[0.01,1]
	T_{min}	5	[0,15]	$fW_{Weibull}$	K	1.5	[0.05,20]
$fVPD_{Horn}$	W_I	5	[0.1,58]	$fW_{Weibull}$	A	0.9	[0,2]

	k_w	5	[0.01,30]	fL_{TAL}	I	0.04	[0,1]
	A	0.29	[0,0.9]	fCI_{EXP}	M	5	[0.001,30]
$fVPD_{MOD17}$	VPD_{max}	20	[10,50]	fCI_{Horn}	R_{opt}	0.5	[0,1]
	VPD_{min}	10	[2,40]		k_c	0.5	[0.01,5]
$fVPD_{PRELES}$	K	-0.005	[-1,-0.001]	fCI_{Wang}	M	0.46	[0,1]
	c_K	0.4	[-50,10]	WAI	AWC	1	[1,1000]
	Ca_0	380	[340,390]		θ	0.05	[0.001,0.2]
	c_m	2000	[100,4000]				
]				

182 **Table S 5. List of bioclimatic variables (Xu et al., 2011) and vegetation index features according to the**
 183 **algorithms of BIO1-BIO11**

Variables	Definitions
BIO1	Annual Mean Temperature
BIO2	Mean Diurnal Range (Mean of monthly maximum temperature minus minimum temperature)
BIO3	Isothermality (BIO2 divided by BIO7 and 100)
BIO4	Temperature Seasonality (standard deviation of temperature multiply with 100)
BIO5	Max Temperature of Warmest Month
BIO6	Min Temperature of Coldest Month
BIO7	Temperature Annual Range (BIO5 minus BIO6)
BIO8	Mean Temperature of Wettest Quarter
BIO9	Mean Temperature of Driest Quarter
BIO10	Mean Temperature of Warmest Quarter
BIO11	Mean Temperature of Coldest Quarter
BIO12	Annual Precipitation
BIO13	Precipitation of Wettest Month
BIO14	Precipitation of Driest Month
BIO15	Precipitation Seasonality (Coefficient of Variation)
BIO16	Precipitation of Wettest Quarter
BIO17	Precipitation of Driest Quarter
BIO18	Precipitation of Warmest Quarter
BIO19	Precipitation of Coldest Quarter
VIF1	Annual mean EVI (enhanced vegetation index)
VIF2	Mean monthly EVI range
VIF3	Mean EVI variability (VIF2 divided by VIF7)

VIF4	EVI seasonality (standard deviation of EVI)
VIF5	Max EVI of Warmest Month
VIF6	Min EVI of Coldest Month
VIF7	Annual EVI Range (BIO5 minus BIO6)
VIF8	Mean EVI of Wettest Quarter
VIF9	Mean EVI of Driest Quarter
VIF10	Mean EVI of Warmest Quarter
VIF11	Mean EVI of Coldest Quarter

184

Table S 6. List of soil properties

Name	Definition
BDRICM	Depth to bedrock (R horizon) up to 200 cm
BDRLOG	Probability of occurrence (0-100%) of R horizon
BDTICM	Absolute depth to bedrock (in cm)
BLDFIE	Bulk density (fine earth) in kg/m ³ at depth 0.00 m
CECSOL	Cation exchange capacity of soil in cmol/kg at depth 0.00 m
CLYPPT	Clay content (0-2 micro meter) mass fraction in % at depth 0.00 m
CRFVOL	Coarse fragments volumetric in % at depth 0.00 m
ORCDRC	Soil organic carbon content (fine earth fraction) in g/kg at depth 0.00 m
PHIOX	Soil pH*10 in H ₂ O at depth 0.00 m
PHIKCL	Soil PH (multy with 10) in KCl at depth 0.00 m
SLTPPT	Silt content (2-50 micro meter) mass fraction in % at depth 0.00 m
SNDPPT	Sand content (50-2000 micro meter) mass fraction in % at depth 0.00 m
AWCh1	Derived available soil water capacity (volumetric fraction) with FC = pF 2.0 for depth 0 cm
AWCh2	Derived available soil water capacity (volumetric fraction) with FC = pF 2.3 for depth 0 cm
AWCh3	Derived available soil water capacity (volumetric fraction) with FC = pF 2.5 for depth 0 cm
WWP	Derived available soil water capacity (volumetric fraction) until wilting point for depth 0 cm
AWCtS	Derived saturated water content (volumetric fraction) teta-S for depth 0 cm

185

186 **Reference**

- 187 Acosta, M., Pavelka, M., Montagnani, L., Kutsch, W., Lindroth, A., Juszczak, R., & Janouš, D. (2013). Soil surface
188 CO₂ efflux measurements in Norway spruce forests: Comparison between four different sites across
189 Europe — from boreal to alpine forest. *Geoderma*, 192, 295-303.
190 doi:<https://doi.org/10.1016/j.geoderma.2012.08.027>
- 191 Ammann, C., Spirig, C., Leifeld, J., & Neftel, A. (2009). Assessment of the nitrogen and carbon budget of two
192 managed temperate grassland fields. *Agriculture, Ecosystems & Environment*, 133(3), 150-162.
193 doi:<https://doi.org/10.1016/j.agee.2009.05.006>
- 194 Anthoni, P. M., Knohl, A., Rebmann, C., Freibauer, A., Mund, M., Ziegler, W., . . . Schulze, E.-D. (2004a). Forest
195 and agricultural land-use-dependent CO₂ exchange in Thuringia, Germany. *Global change biology*, 10(12),
196 2005-2019. doi:<https://doi.org/10.1111/j.1365-2486.2004.00863.x>
- 197 Anthoni, P. M., Knohl, A., Rebmann, C., Freibauer, A., Mund, M., Ziegler, W., . . . Schulze, E. D. (2004b). Forest
198 and agricultural land-use-dependent CO₂ exchange in Thuringia, Germany. *Global change biology*,
199 10(12), 2005-2019. doi:10.1111/j.1365-2486.2004.00863.X
- 200 Arain, M. A., & Restrepo-Coupe, N. (2005). Net ecosystem production in a temperate pine plantation in
201 southeastern Canada. *Agricultural and Forest Meteorology*, 128(3-4), 223-241.
- 202 Archibald, S. A., Kirton, A., van der Merwe, M. R., Scholes, R. J., Williams, C. A., & Hanan, N. (2009). Drivers of
203 inter-annual variability in Net Ecosystem Exchange in a semi-arid savanna ecosystem, South Africa.
204 *Biogeosciences*, 6(2), 251-266. doi:10.5194/bg-6-251-2009
- 205 Ardö, J., Mölder, M., El-Tahir, B. A., & Elkhidir, H. A. M. (2008). Seasonal variation of carbon fluxes in a sparse
206 savanna in semi arid Sudan. *Carbon Balance and Management*, 3(1), 7. doi:10.1186/1750-0680-3-7
- 207 Arneth, A., Kurbatova, J., Kolle, O., Shibalova, O. B., Lloyd, J., Vygodskaya, N. N., & Schulze, E. D. (2002).
208 Comparative ecosystem-atmosphere exchange of energy and mass in a European Russian and a central
209 Siberian bog II. Interseasonal and interannual variability of CO₂ fluxes. *Tellus B: Chemical and Physical
210 Meteorology*, 54(5), 514-530. doi:10.3402/tellusb.v54i5.16684
- 211 Aubinet, M., Moureaux, C., Bodson, B., Dufranne, D., Heinesch, B., Suleau, M., . . . Vilret, A. (2009). Carbon
212 sequestration by a crop over a 4-year sugar beet/winter wheat/seed potato/winter wheat rotation cycle.
213 *Agricultural and Forest Meteorology*, 149(3-4), 407-418.
- 214 Aurela, M., Lohila, A., Tuovinen, J. P., Hatakka, J., Penttilä, T., & Laurila, T. (2015). Carbon dioxide and energy
215 flux measurements in four northern-boreal ecosystems at Pallas. *Boreal Environment Research*, 20(4), 455-
216 473. Retrieved from <Go to ISI>://WOS:000361411500002
- 217 AURELA, M., RIUTTA, T., LAURILA, T., TUOVINEN, J.-P., VESALA, T., TUITTIILA, E.-S., . . . LAINE, J.
218 (2007). CO₂ exchange of a sedge fen in southern Finland—the impact of a drought period. *Tellus B*, 59(5),
219 826-837. doi:<https://doi.org/10.1111/j.1600-0889.2007.00309.x>
- 220 Baldocchi, D. D., Vogel, C. A., & Hall, B. (1997). Seasonal variation of carbon dioxide exchange rates above and
221 below a boreal jack pine forest. *Agricultural and Forest Meteorology*, 83(1-2), 147-170.
- 222 Belletti Marchesini, L., Papale, D., Reichstein, M., Vuichard, N., Tchebakova, N., & Valentini, R. (2007). Carbon
223 balance assessment of a natural steppe of southern Siberia by multiple constraint approach. *Biogeosciences*,
224 4(4), 581-595. doi:10.5194/bg-4-581-2007

- 225 Berbigier, P., Bonnefond, J.-M., & Mellmann, P. (2001). CO₂ and water vapour fluxes for 2 years above Euroflux
226 forest site. *Agricultural and Forest Meteorology*, 108(3), 183-197. doi:[https://doi.org/10.1016/S0168-1923\(01\)00240-4](https://doi.org/10.1016/S0168-1923(01)00240-4)
- 228 Bergeron, O., Margolis, H. A., Black, T. A., Coursolle, C., Dunn, A. L., Barr, A. G., & Wofsy, S. C. (2007).
229 Comparison of carbon dioxide fluxes over three boreal black spruce forests in Canada. *Global change
230 biology*, 13(1), 89-107.
- 231 Beringer, J., Hacker, J., Hutley, L. B., Leuning, R., Arndt, S. K., Amiri, R., . . . Hensley, C. (2011). SPECIAL—
232 Savanna patterns of energy and carbon integrated across the landscape. *Bulletin of the American
233 Meteorological Society*, 92(11), 1467-1485.
- 234 Beringer, J., Hutley, L. B., McHugh, I., Arndt, S. K., Campbell, D., Cleugh, H. A., . . . Evans, B. (2016). An
235 introduction to the Australian and New Zealand flux tower network—OzFlux. *Biogeosciences*, 13(21), 5895-
236 5916.
- 237 Beringer, J., Hutley, L. B., Tapper, N. J., Coutts, A., Kerley, A., & O'Grady, A. P. (2003). Fire impacts on surface
238 heat, moisture and carbon fluxes from a tropical savanna in northern Australia. *International Journal of
239 Wildland Fire*, 12(4), 333-340.
- 240 Bernhofer, C., Aubinet, M., Clement, R., Grelle, A., Grünwald, T., Ibrom, A., . . . Tenhunen, J. D. (2003). Spruce
241 Forests (Norway and Sitka Spruce, Including Douglas Fir): Carbon and Water Fluxes and Balances,
242 Ecological and Ecophysiological Determinants. In R. Valentini (Ed.), *Fluxes of Carbon, Water and Energy
243 of European Forests* (pp. 99-123). Berlin, Heidelberg: Springer Berlin Heidelberg.
- 244 Billesbach D, B. J., Torn M. (2016). *FLUXNET2015 US-ARI ARM USDA UNL OSU Woodward Switchgrass 1*.
245 Retrieved from FluxNet; Lawerence Berkeley National Lab; US Department of Agriculture; Univ. of
246 Nebraska, Lincoln, NE (United States):
- 247 Black, T., Den Hartog, G., Neumann, H., Blanken, P., Yang, P., Russell, C., . . . Staebler, R. (1996). Annual cycles
248 of water vapour and carbon dioxide fluxes in and above a boreal aspen forest. *Global change biology*, 2(3),
249 219-229.
- 250 Bloomfield, K. J., Cernusak, L. A., Eamus, D., Ellsworth, D. S., Colin Prentice, I., Wright, I. J., . . . Cleverly, J.
251 (2018). A continental-scale assessment of variability in leaf traits: Within species, across sites and between
252 seasons. *Functional Ecology*, 32(6), 1492-1506.
- 253 Breiman, L. (2001). Random forests. *Machine learning*, 45(1), 5-32.
- 254 Breiman, L. (2002). Manual on setting up, using, and understanding random forests v3. 1. *Statistics Department
255 University of California Berkeley, CA, USA*, 1, 58.
- 256 Bristow, M., Hutley, L. B., Beringer, J., Livesley, S. J., Edwards, A. C., & Arndt, S. K. (2016). Quantifying the
257 relative importance of greenhouse gas emissions from current and future savanna land use change across
258 northern Australia. *Biogeosciences*, 13(22), 6285-6303.
- 259 Carrara, A., Janssens, I. A., Yuste, J. C., & Ceulemans, R. (2004). Seasonal changes in photosynthesis, respiration
260 and NEE of a mixed temperate forest. *Agricultural and Forest Meteorology*, 126(1-2), 15-31.
- 261 Chen, S., Chen, J., Lin, G., Zhang, W., Miao, H., Wei, L., . . . Han, X. (2009). Energy balance and partition in Inner
262 Mongolia steppe ecosystems with different land use types. *Agricultural and Forest Meteorology*, 149(11),
263 1800-1809. doi:<https://doi.org/10.1016/j.agrformet.2009.06.009>

- 264 Chiesi, M., Maselli, F., Bindi, M., Fibbi, L., Cherubini, P., Arlotta, E., . . . Seufert, G. (2005). Modelling carbon
265 budget of Mediterranean forests using ground and remote sensing measurements. *Agricultural and Forest*
266 *Meteorology*, 135(1), 22-34. doi:<https://doi.org/10.1016/j.agrformet.2005.09.011>
- 267 Clark, K. L., Gholz, H. L., Moncrieff, J. B., Cropley, F., & Loescher, H. W. (1999). ENVIRONMENTAL
268 CONTROLS OVER NET EXCHANGES OF CARBON DIOXIDE FROM CONTRASTING FLORIDA
269 ECOSYSTEMS. *Ecological Applications*, 9(3), 936-948. doi:[https://doi.org/10.1890/1051-0761\(1999\)009\[0936:ECONEO\]2.0.CO;2](https://doi.org/10.1890/1051-0761(1999)009[0936:ECONEO]2.0.CO;2)
- 270
- 271 Cleverly, J., Boulain, N., Villalobos-Vega, R., Grant, N., Faux, R., Wood, C., . . . Eamus, D. (2013). Dynamics of
272 component carbon fluxes in a semi-arid Acacia woodland, central Australia. *Journal of Geophysical*
273 *Research: Biogeosciences*, 118(3), 1168-1185.
- 274 Cleverly, J., Eamus, D., Van Gorsel, E., Chen, C., Rumman, R., Luo, Q., . . . Huete, A. (2016). Productivity and
275 evapotranspiration of two contrasting semiarid ecosystems following the 2011 global carbon land sink
276 anomaly. *Agricultural and Forest Meteorology*, 220, 151-159.
277 doi:<https://doi.org/10.1016/j.agrformet.2016.01.086>
- 278 Cook, B. D., Davis, K. J., Wang, W., Desai, A., Berger, B. W., Teclaw, R. M., . . . Heilman, W. (2004). Carbon
279 exchange and venting anomalies in an upland deciduous forest in northern Wisconsin, USA. *Agricultural*
280 *and Forest Meteorology*, 126(3), 271-295. doi:<https://doi.org/10.1016/j.agrformet.2004.06.008>
- 281 Coursolle, C., Margolis, H., Giasson, M.-A., Bernier, P.-Y., Amiro, B., Arain, M., . . . McCaughey, J. (2012).
282 Influence of stand age on the magnitude and seasonality of carbon fluxes in Canadian forests. *Agricultural*
283 *and Forest Meteorology*, 165, 136-148.
- 284 D., B. (2016). *AmeriFlux US-Cop Corral Pocket*. Retrieved from Lawrence Berkeley National Lab.(LBNL),
285 Berkeley, CA (United States). AmeriFlux; Univ. of Utah, Salt Lake City, UT (United States):
- 286 Da Rocha, H. R., Manzi, A. O., Cabral, O. M., Miller, S. D., Goulden, M. L., Saleska, S. R., . . . Artaxo, P. (2009).
287 Patterns of water and heat flux across a biome gradient from tropical forest to savanna in Brazil. *Journal of*
288 *Geophysical Research: Biogeosciences*, 114(G1).
- 289 DeForest, J. L., Noormets, A., McNulty, S. G., Sun, G., Tenney, G., & Chen, J. (2006). Phenophases alter the soil
290 respiration-temperature relationship in an oak-dominated forest. *International Journal of Biometeorology*,
291 51(2), 135-144. doi:10.1007/s00484-006-0046-7
- 292 Desai, A. R., Bolstad, P. V., Cook, B. D., Davis, K. J., & Carey, E. V. (2005). Comparing net ecosystem exchange
293 of carbon dioxide between an old-growth and mature forest in the upper Midwest, USA. *Agricultural and*
294 *Forest Meteorology*, 128(1), 33-55. doi:<https://doi.org/10.1016/j.agrformet.2004.09.005>
- 295 Dolman, A. J., Moors, E. J., & Elbers, J. A. (2002). The carbon uptake of a mid latitude pine forest growing on
296 sandy soil. *Agricultural and Forest Meteorology*, 111(3), 157-170. doi:[https://doi.org/10.1016/S0168-1923\(02\)00024-2](https://doi.org/10.1016/S0168-1923(02)00024-2)
- 297
- 298 DON, A., REBMANN, C., KOLLE, O., SCHERER-LORENZEN, M., & SCHULZE, E.-D. (2009). Impact of
299 afforestation-associated management changes on the carbon balance of grassland. *Global change biology*,
300 15(8), 1990-2002. doi:<https://doi.org/10.1111/j.1365-2486.2009.01873.x>
- 301 Dušek, J., Čížková, H., Stellner, S., Czerný, R., & Květ, J. (2012). Fluctuating water table affects gross ecosystem
302 production and gross radiation use efficiency in a sedge-grass marsh. *Hydrobiologia*, 692(1), 57-66.
303 doi:10.1007/s10750-012-0998-z

- 304 Epstein, H. E., Calef, M. P., Walker, M. D., Stuart Chapin III, F., & Starfield, A. M. (2004). Detecting changes in
305 arctic tundra plant communities in response to warming over decadal time scales. *Global change biology*,
306 10(8), 1325-1334. doi:<https://doi.org/10.1111/j.1529-8817.2003.00810.x>
- 307 Ferréa, C., Zenone, T., Comolli, R., & Seufert, G. (2012). Estimating heterotrophic and autotrophic soil respiration
308 in a semi-natural forest of Lombardy, Italy. *Pedobiologia*, 55(6), 285-294.
309 doi:<https://doi.org/10.1016/j.pedobi.2012.05.001>
- 310 Flanagan, L. B., Wever, L. A., & Carlson, P. J. (2002). Seasonal and interannual variation in carbon dioxide
311 exchange and carbon balance in a northern temperate grassland. *Global change biology*, 8(7), 599-615.
- 312 Flechard, C. R., Oijen, M. v., Cameron, D. R., Vries, W. d., Ibrom, A., Buchmann, N., . . . Montagnani, L. (2020).
313 Carbon–nitrogen interactions in European forests and semi-natural vegetation–Part 2: Untangling climatic,
314 edaphic, management and nitrogen deposition effects on carbon sequestration potentials. *Biogeosciences*,
315 17(6), 1621-1654.
- 316 Galvagno, M., Wohlfahrt, G., Cremonese, E., Rossini, M., Colombo, R., Filippa, G., . . . Migliavacca, M. (2013).
317 Phenology and carbon dioxide source/sink strength of a subalpine grassland in response to an exceptionally
318 short snow season. *Environmental Research Letters*, 8(2). doi:10.1088/1748-9326/8/2/025008
- 319 Giasson, M.-A., Coursolle, C., & Margolis, H. A. (2006). Ecosystem-level CO₂ fluxes from a boreal cutover in
320 eastern Canada before and after scarification. *Agricultural and Forest Meteorology*, 140(1-4), 23-40.
- 321 Gilmanov, T. G., Tieszen, L. L., Wylie, B. K., Flanagan, L. B., Frank, A. B., Haferkamp, M. R., . . . Morgan, J. A.
322 (2005). Integration of CO₂ flux and remotely-sensed data for primary production and ecosystem respiration
323 analyses in the Northern Great Plains: potential for quantitative spatial extrapolation. *Global Ecology and*
324 *Biogeography*, 14(3), 271-292. doi:<https://doi.org/10.1111/j.1466-822X.2005.00151.x>
- 325 Goldstein, A. H., Hultman, N. E., Fracheboud, J. M., Bauer, M. R., Panek, J. A., Xu, M., . . . Baugh, W. (2000).
326 Effects of climate variability on the carbon dioxide, water, and sensible heat fluxes above a ponderosa pine
327 plantation in the Sierra Nevada (CA). *Agricultural and Forest Meteorology*, 101(2), 113-129.
328 doi:[https://doi.org/10.1016/S0168-1923\(99\)00168-9](https://doi.org/10.1016/S0168-1923(99)00168-9)
- 329 Gough, C. M., Vogel, C. S., Schmid, H. P., Su, H. B., & Curtis, P. S. (2008). Multi-year convergence of biometric
330 and meteorological estimates of forest carbon storage. *Agricultural and Forest Meteorology*, 148(2), 158-
331 170. doi:<https://doi.org/10.1016/j.agrformet.2007.08.004>
- 332 Granier, A., Ceschia, E., Damesin, C., Dufrêne, E., Epron, D., Gross, P., . . . Saugier, B. (2000). The carbon balance
333 of a young Beech forest. *Functional Ecology*, 14(3), 312-325. doi:<https://doi.org/10.1046/j.1365-2435.2000.00434.x>
- 335 Griebel, A., Bennett, L. T., Metzen, D., Cleverly, J., Burba, G., & Arndt, S. K. (2016). Effects of inhomogeneities
336 within the flux footprint on the interpretation of seasonal, annual, and interannual ecosystem carbon
337 exchange. *Agricultural and Forest Meteorology*, 221, 50-60.
- 338 Gu, L., Pallardy, S. G., Yang, B., Hosman, K. P., Mao, J., Ricciuto, D., . . . Sun, Y. (2016). Testing a land model in
339 ecosystem functional space via a comparison of observed and modeled ecosystem flux responses to
340 precipitation regimes and associated stresses in a Central U.S. forest. *Journal of Geophysical Research: Biogeosciences*, 121(7), 1884-1902. doi:<https://doi.org/10.1002/2015JG003302>
- 342 Hao, Y., Baik, J., & Choi, M. (2019). Developing a soil water index-based Priestley–Taylor algorithm for estimating
343 evapotranspiration over East Asia and Australia. *Agricultural and Forest Meteorology*, 279, 107760.

- 344 Heinsch, F. A., Heilman, J. L., McInnes, K. J., Cobos, D. R., Zuberer, D. A., & Roelke, D. L. (2004). Carbon
 345 dioxide exchange in a high marsh on the Texas Gulf Coast: effects of freshwater availability. *Agricultural*
 346 *and Forest Meteorology*, 125(1), 159-172. doi:<https://doi.org/10.1016/j.agrformet.2004.02.007>
- 347 Hollinger, D. Y., Goltz, S. M., Davidson, E. A., Lee, J. T., Tu, K., & Valentine, H. T. (1999). Seasonal patterns and
 348 environmental control of carbon dioxide and water vapour exchange in an ecotonal boreal forest. *Global*
 349 *change biology*, 5(8), 891-902. doi:<https://doi.org/10.1046/j.1365-2486.1999.00281.x>
- 350 Hommeltenberg, J., Schmid, H. P., Drösler, M., & Werle, P. (2014). Can a bog drained for forestry be a stronger
 351 carbon sink than a natural bog forest? *Biogeosciences*, 11(13), 3477-3493. doi:10.5194/bg-11-3477-2014
- 352 Horn, J., & Schulz, K. (2011). Identification of a general light use efficiency model for gross primary production.
 353 *Biogeosciences*, 8(4), 999.
- 354 Howard, E. A., Gower, S. T., Foley, J. A., & Kucharik, C. J. (2004). Effects of logging on carbon dynamics of a jack
 355 pine forest in Saskatchewan, Canada. *Global change biology*, 10(8), 1267-1284.
- 356 Humphreys, E. R., Black, T. A., Morgenstern, K., Cai, T., Drewitt, G. B., Nesic, Z., & Trofymow, J. (2006). Carbon
 357 dioxide fluxes in coastal Douglas-fir stands at different stages of development after clearcut harvesting.
 358 *Agricultural and Forest Meteorology*, 140(1-4), 6-22.
- 359 Hutley, L. B., Beringer, J., Isaac, P. R., Hacker, J. M., & Cernusak, L. A. (2011). A sub-continental scale living
 360 laboratory: Spatial patterns of savanna vegetation over a rainfall gradient in northern Australia.
 361 *Agricultural and Forest Meteorology*, 151(11), 1417-1428.
- 362 Ikawa, H., Nakai, T., Busey, R. C., Kim, Y., Kobayashi, H., Nagai, S., . . . Hinzman, L. (2015). Understory CO₂,
 363 sensible heat, and latent heat fluxes in a black spruce forest in interior Alaska. *Agricultural and Forest*
 364 *Meteorology*, 214-215, 80-90. doi:<https://doi.org/10.1016/j.agrformet.2015.08.247>
- 365 Imer, D., Merbold, L., Eugster, W., & Buchmann, N. (2013). Temporal and spatial variations of soil
 366 CO₂, CH₄ and N₂O fluxes at three differently managed grasslands.
 367 *Biogeosciences*, 10(9), 5931-5945. doi:10.5194/bg-10-5931-2013
- 368 Jacobs, C. M. J., Jacobs, A. F. G., Bosveld, F. C., Hendriks, D. M. D., Hensen, A., Kroon, P. S., . . . Veenendaal, E.
 369 M. (2007). Variability of annual CO₂ exchange from Dutch grasslands. *Biogeosciences*, 4(5),
 370 803-816. doi:10.5194/bg-4-803-2007
- 371 Jarvis, P., Massheder, J., Hale, S., Moncrieff, J., Rayment, M., & Scott, S. (1997). Seasonal variation of carbon
 372 dioxide, water vapor, and energy exchanges of a boreal black spruce forest. *Journal of Geophysical*
 373 *Research: Atmospheres*, 102(D24), 28953-28966.
- 374 Kalliokoski, T., Makela, A., Fronzek, S., Minunno, F., & Peltoniemi, M. (2018). Decomposing sources of
 375 uncertainty in climate change projections of boreal forest primary production. *Agricultural and Forest*
 376 *Meteorology*, 262, 192-205. doi:10.1016/j.agrformet.2018.06.030
- 377 Knohl, A., Schulze, E.-D., Kolle, O., & Buchmann, N. (2003). Large carbon uptake by an unmanaged 250-year-old
 378 deciduous forest in Central Germany. *Agricultural and Forest Meteorology*, 118(3), 151-167.
 379 doi:[https://doi.org/10.1016/S0168-1923\(03\)00115-1](https://doi.org/10.1016/S0168-1923(03)00115-1)
- 380 Koskinen, M., Minkkinen, K., Ojanen, P., Kämäräinen, M., Laurila, T., & Lohila, A. (2014). Measurements of
 381 CO₂ exchange with an automated chamber system throughout the year: challenges in
 382 measuring night-time respiration on porous peat soil. *Biogeosciences*, 11(2), 347-363. doi:10.5194/bg-11-
 383 347-2014

- 384 Krupková, L., Marková, I., Havránková, K., Pokorný, R., Urban, O., Šigut, L., . . . Marek, M. V. (2017).
385 Comparison of different approaches of radiation use efficiency of biomass formation estimation in
386 Mountain Norway spruce. *Trees*, 31(1), 325-337. doi:10.1007/s00468-016-1486-2
- 387 Kurbatova, J., Li, C., Varlagin, A., Xiao, X., & Vygodskaya, N. (2008). Modeling carbon dynamics in two adjacent
388 spruce forests with different soil conditions in Russia. *Biogeosciences*, 5(4), 969-980. doi:10.5194/bg-5-
389 969-2008
- 390 Kwon, H., Law, B. E., Thomas, C. K., & Johnson, B. G. (2018). The influence of hydrological variability on
391 inherent water use efficiency in forests of contrasting composition, age, and precipitation regimes in the
392 Pacific Northwest. *Agricultural and Forest Meteorology*, 249, 488-500.
393 doi:<https://doi.org/10.1016/j.agrformet.2017.08.006>
- 394 Lafleur, P. M., Roulet, N. T., Bubier, J. L., Frolking, S., & Moore, T. R. (2003). Interannual variability in the
395 peatland-atmosphere carbon dioxide exchange at an ombrotrophic bog. *Global Biogeochemical Cycles*,
396 17(2).
- 397 Law, B. E., Thornton, P. E., Irvine, J., Anthoni, P. M., & Van Tuyl, S. (2001). Carbon storage and fluxes in
398 ponderosa pine forests at different developmental stages. *Global change biology*, 7(7), 755-777.
399 doi:<https://doi.org/10.1046/j.1365-1013.2001.00439.x>
- 400 Leuning, R., Cleugh, H. A., Zegelin, S. J., & Hughes, D. (2005). Carbon and water fluxes over a temperate
401 Eucalyptus forest and a tropical wet/dry savanna in Australia: measurements and comparison with MODIS
402 remote sensing estimates. *Agricultural and Forest Meteorology*, 129(3-4), 151-173.
- 403 Lipson, D. A., Wilson, R. F., & Oechel, W. C. (2005). Effects of Elevated Atmospheric CO₂ on Soil
404 Microbial Biomass, Activity, and Diversity in a Chaparral Ecosystem. *Applied and Environmental
405 Microbiology*, 71(12), 8573-8580. doi:10.1128/aem.71.12.8573-8580.2005
- 406 López-Ballesteros, A., Serrano-Ortiz, P., Kowalski, A. S., Sánchez-Cañete, E. P., Scott, R. L., & Domingo, F.
407 (2017). Subterranean ventilation of allochthonous CO₂ governs net CO₂ exchange in a semiarid
408 Mediterranean grassland. *Agricultural and Forest Meteorology*, 234-235, 115-126.
409 doi:<https://doi.org/10.1016/j.agrformet.2016.12.021>
- 410 Loubet, B., Laville, P., Lehuger, S., Larmanou, E., Flechard, C., Mascher, N., . . . Cellier, P. (2011). Carbon,
411 nitrogen and Greenhouse gases budgets over a four years crop rotation in northern France. *Plant and Soil*,
412 343(1-2), 109-137. doi:10.1007/s11104-011-0751-9
- 413 Lund, M., Falk, J. M., Friberg, T., Mbufong, H. N., Sigsgaard, C., Soegaard, H., & Tamstorf, M. P. (2012). Trends
414 in CO₂ exchange in a high Arctic tundra heath, 2000–2010. *Journal of Geophysical Research: Biogeosciences*, 117(G2). doi:<https://doi.org/10.1029/2011JG001901>
- 416 Ma, S., Baldocchi, D., Wolf, S., & Verfaillie, J. (2016). Slow ecosystem responses conditionally regulate annual
417 carbon balance over 15 years in Californian oak-grass savanna. *Agricultural and Forest Meteorology*, 228-
418 229, 252-264. doi:<https://doi.org/10.1016/j.agrformet.2016.07.016>
- 419 Ma, S., Baldocchi, D. D., Mambelli, S., & Dawson, T. E. (2011). Are temporal variations of leaf traits responsible
420 for seasonal and inter-annual variability in ecosystem CO₂ exchange? *Functional Ecology*, 25(1), 258-270.
421 doi:<https://doi.org/10.1111/j.1365-2435.2010.01779.x>
- 422 Mäkelä, A., Pulkkinen, M., Kolari, P., Lagergren, F., Berbigier, P., Lindroth, A., . . . Hari, P. (2008). Developing an
423 empirical model of stand GPP with the LUE approach: analysis of eddy covariance data at five contrasting
424 conifer sites in Europe. *Global change biology*, 14(1), 92-108.

- 425 Marcolla, B., Cescatti, A., Montagnani, L., Manca, G., Kerschbaumer, G., & Minerbi, S. (2005). Importance of
 426 advection in the atmospheric CO₂ exchanges of an alpine forest. *Agricultural and Forest Meteorology*,
 427 130(3), 193-206. doi:<https://doi.org/10.1016/j.agrformet.2005.03.006>
- 428 Marcolla, B., Pitacco, A., & Cescatti, A. (2003). Canopy Architecture and Turbulence Structure in a Coniferous
 429 Forest. *Boundary-Layer Meteorology*, 108(1), 39-59. doi:10.1023/A:1023027709805
- 430 Merbold, L., Ardö, J., Arneth, A., Scholes, R. J., Nouvellon, Y., de Grandcourt, A., . . . Kutsch, W. L. (2009).
 431 Precipitation as driver of carbon fluxes in 11 African ecosystems. *Biogeosciences*, 6(6), 1027-1041.
 432 doi:10.5194/bg-6-1027-2009
- 433 Merbold, L., Eugster, W., Stieger, J., Zahniser, M., Nelson, D., & Buchmann, N. (2014). Greenhouse gas budget
 434 (CO₂, CH₄ and N₂O) of intensively managed grassland following restoration. *Global change biology*,
 435 20(6), 1913-1928.
- 436 Meyer, W., Kondrlovà, E., & Koerber, G. (2015). Evaporation of perennial semi-arid woodland in southeastern
 437 Australia is adapted for irregular but common dry periods. *Hydrological Processes*, 29(17), 3714-3726.
- 438 Michelot, A., Eglin, T., Dufrene, E., Lelarge-Trouverie, C., & Damesin, C. (2011). Comparison of seasonal
 439 variations in water-use efficiency calculated from the carbon isotope composition of tree rings and flux data
 440 in a temperate forest. *Plant Cell and Environment*, 34(2), 230-244. doi:10.1111/j.1365-3040.2010.02238.x
- 441 Migliavacca, M., Meroni, M., Manca, G., Matteucci, G., Montagnani, L., Grassi, G., . . . Seufert, G. (2009).
 442 Seasonal and interannual patterns of carbon and water fluxes of a poplar plantation under peculiar eco-
 443 climatic conditions. *Agricultural and Forest Meteorology*, 149(9), 1460-1476.
 444 doi:<https://doi.org/10.1016/j.agrformet.2009.04.003>
- 445 Mkhabela, M., Amiro, B., Barr, A., Black, T., Hawthorne, I., Kidston, J., . . . Sass, A. (2009). Comparison of carbon
 446 dynamics and water use efficiency following fire and harvesting in Canadian boreal forests. *Agricultural
 447 and Forest Meteorology*, 149(5), 783-794.
- 448 Monson, R. K., Turnipseed, A. A., Sparks, J. P., Harley, P. C., Scott-Denton, L. E., Sparks, K., & Huxman, T. E.
 449 (2002). Carbon sequestration in a high-elevation, subalpine forest. *Global change biology*, 8(5), 459-478.
 450 doi:<https://doi.org/10.1046/j.1365-2486.2002.00480.x>
- 451 Nakai, T., Kim, Y., Busey, R. C., Suzuki, R., Nagai, S., Kobayashi, H., . . . Ito, A. (2013). Characteristics of
 452 evapotranspiration from a permafrost black spruce forest in interior Alaska. *Polar Science*, 7(2), 136-148.
 453 doi:<https://doi.org/10.1016/j.polar.2013.03.003>
- 454 Nardino, M., Georgiadis, T., Rossi, F., Ponti, F., Miglietta, F. & Magliulo, V. (2002). *Primary productivity and
 455 evapotranspiration of a mixed forest*. Paper presented at the Congress CNR-ISA Fo., Istituto per i Sistemi
 456 Agricoli e Forestali del Mediterraneo, Portici.
- 457 Noormets, A., Chen, J., & Crow, T. R. (2007). Age-Dependent Changes in Ecosystem Carbon Fluxes in Managed
 458 Forests in Northern Wisconsin, USA. *Ecosystems*, 10(2), 187-203. doi:10.1007/s10021-007-9018-y
- 459 Noormets, A., McNulty, S. G., Domec, J.-C., Gavazzi, M., Sun, G., & King, J. S. (2012). The role of harvest residue
 460 in rotation cycle carbon balance in loblolly pine plantations. Respiration partitioning approach. *Global
 461 change biology*, 18(10), 3186-3201. doi:<https://doi.org/10.1111/j.1365-2486.2012.02776.x>
- 462 Ouimette, A. P., Ollinger, S. V., Richardson, A. D., Hollinger, D. Y., Keenan, T. F., Lepine, L. C., & Vadeboncoeur,
 463 M. A. (2018). Carbon fluxes and interannual drivers in a temperate forest ecosystem assessed through
 464 comparison of top-down and bottom-up approaches. *Agricultural and Forest Meteorology*, 256-257, 420-
 465 430. doi:<https://doi.org/10.1016/j.agrformet.2018.03.017>

- 466 Papale, D., Migliavacca, M., Cremonese, E., Cescatti, A., Alberti, G., Balzarolo, M., . . . Valentini, R. (2015).
467 Carbon, Water and Energy Fluxes of Terrestrial Ecosystems in Italy. In R. Valentini & F. Miglietta (Eds.),
468 *The Greenhouse Gas Balance of Italy: An Insight on Managed and Natural Terrestrial Ecosystems* (pp. 11-
469 45). Berlin, Heidelberg: Springer Berlin Heidelberg.
- 470 Pastorello, G., Trotta, C., Canfora, E., Chu, H., Christianson, D., Cheah, Y.-W., . . . Humphrey, M. (2020). The
471 FLUXNET2015 dataset and the ONEFlux processing pipeline for eddy covariance data. *Scientific data*,
472 7(1), 1-27.
- 473 Peichl, M., & Arain, M. A. (2007). Allometry and partitioning of above-and belowground tree biomass in an age-
474 sequence of white pine forests. *Forest Ecology and Management*, 253(1-3), 68-80.
- 475 Pejam, M., Arain, M., & McCaughey, J. (2006). Energy and water vapour exchanges over a mixedwood boreal
476 forest in Ontario, Canada. *Hydrological Processes*, 20(17), 3709-3724.
- 477 Pereira, J. S., Mateus, J. A., Aires, L. M., Pita, G., Pio, C., David, J. S., . . . Rodrigues, A. (2007). Net ecosystem
478 carbon exchange in three contrasting Mediterranean ecosystems – the effect of drought.
479 *Biogeosciences*, 4(5), 791-802. doi:10.5194/bg-4-791-2007
- 480 Perez-Priego, O., El-Madany, T. S., Migliavacca, M., Kowalski, A. S., Jung, M., Carrara, A., . . . Reichstein, M.
481 (2017). Evaluation of eddy covariance latent heat fluxes with independent lysimeter and sapflow estimates
482 in a Mediterranean savannah ecosystem. *Agricultural and Forest Meteorology*, 236, 87-99.
483 doi:<https://doi.org/10.1016/j.agrformet.2017.01.009>
- 484 Pilegaard, K., & Ibrom, A. (2020). Net carbon ecosystem exchange during 24 years in the Sorø Beech Forest—
485 relations to phenology and climate. *Tellus B: Chemical and Physical Meteorology*, 72(1), 1-17.
- 486 Powell, T. L., Bracho, R., Li, J., Dore, S., Hinkle, C. R., & Drake, B. G. (2006). Environmental controls over net
487 ecosystem carbon exchange of scrub oak in central Florida. *Agricultural and Forest Meteorology*, 141(1),
488 19-34. doi:<https://doi.org/10.1016/j.agrformet.2006.09.002>
- 489 Prescher, A.-K., Grünwald, T., & Bernhofer, C. (2010). Land use regulates carbon budgets in eastern Germany:
490 From NEE to NBP. *Agricultural and Forest Meteorology*, 150(7), 1016-1025.
491 doi:10.1016/J.AGRFORMAT.2010.03.008
- 492 Rambal, S., Joffre, R., Ourcival, J. M., Cavender-Bares, J., & Rocheteau, A. (2004). The growth respiration
493 component in eddy CO₂ flux from a *Quercus ilex* mediterranean forest. *Global change biology*, 10(9),
494 1460-1469. doi:<https://doi.org/10.1111/j.1365-2486.2004.00819.x>
- 495 Rebmann, C., Zeri, M., Lasslop, G., Mund, M., Kolle, O., Schulze, E.-D., & Feigenwinter, C. (2010). Treatment and
496 assessment of the CO₂-exchange at a complex forest site in Thuringia, Germany. *Agricultural and Forest
497 Meteorology*, 150(5), 684-691. doi:<https://doi.org/10.1016/j.agrformet.2009.11.001>
- 498 Renchon, A. A., Griebel, A., Metzen, D., Williams, C. A., Medlyn, B., Duursma, R. A., . . . Isaac, P. (2018). Upside-
499 down fluxes Down Under: CO₂ net sink in winter and net source in summer in a temperate evergreen
500 broadleaf forest. *Biogeosciences*, 15(12), 3703-3716.
- 501 Reverter, B. R., Sánchez-Cañete, E. P., Resco, V., Serrano-Ortiz, P., Oyonarte, C., & Kowalski, A. S. (2010).
502 Analyzing the major drivers of NEE in a Mediterranean alpine shrubland. *Biogeosciences*, 7(9), 2601-2611.
503 doi:10.5194/bg-7-2601-2010
- 504 Rey, A., Pegoraro, E., Tedeschi, V., De Parri, I., Jarvis, P. G., & Valentini, R. (2002). Annual variation in soil
505 respiration and its components in a coppice oak forest in Central Italy. *Global change biology*, 8(9), 851-
506 866. doi:<https://doi.org/10.1046/j.1365-2486.2002.00521.x>

- 507 Rodrigues, A., Pita, G., Mateus, J., Kurz-Besson, C., Casquilho, M., Cerasoli, S., . . . Pereira, J. (2011). Eight years
508 of continuous carbon fluxes measurements in a Portuguese eucalypt stand under two main events: Drought
509 and felling. *Agricultural and Forest Meteorology*, 151(4), 493-507.
510 doi:<https://doi.org/10.1016/j.agrformet.2010.12.007>
- 511 Roman, D. T., Novick, K. A., Brzostek, E. R., Dragoni, D., Rahman, F., & Phillips, R. P. (2015). The role of
512 isohydric and anisohydric species in determining ecosystem-scale response to severe drought. *Oecologia*,
513 179(3), 641-654. doi:10.1007/s00442-015-3380-9
- 514 Ruehr, N. K., Law, B. E., Quandt, D., & Williams, M. (2014). Effects of heat and drought on carbon and water
515 dynamics in a regenerating semi-arid pine forest: a combined experimental and modeling approach.
516 *Biogeosciences*, 11(15), 4139-4156. doi:10.5194/bg-11-4139-2014
- 517 Running, S. W., Nemani, R. R., Heinsch, F. A., Zhao, M., Reeves, M., & Hashimoto, H. (2004). A continuous
518 satellite-derived measure of global terrestrial primary production. *Bioscience*, 54(6), 547-560.
- 519 Sabbatini, S., Arriga, N., Bertolini, T., Castaldi, S., Chiti, T., Consalvo, C., . . . Papale, D. (2016). Greenhouse gas
520 balance of cropland conversion to bioenergy poplar short-rotation coppice. *Biogeosciences*, 13(1), 95-113.
521 doi:10.5194/bg-13-95-2016
- 522 Sagerfors, J., Lindroth, A., Grelle, A., Klemedtsson, L., Weslien, P., & Nilsson, M. (2008). Annual CO₂ exchange
523 between a nutrient-poor, minerotrophic, boreal mire and the atmosphere. *Journal of Geophysical Research:*
524 *Biogeosciences*, 113(G1). doi:<https://doi.org/10.1029/2006JG000306>
- 525 Sanz M J, C. A., Gimeno C, et al. (2004). *Effects of a dry and warm summer conditions on CO₂ and energy fluxes
526 from three Mediterranean ecosystems*. Paper presented at the Geophys. Res. Abstr.
- 527 Schroder, I. (2014). Arcturus Emerald OzFlux tower site OzFlux: Australian and New Zealand flux research and
528 monitoring. *hdl*, 102(100), 14249.
- 529 Scott, R. L. (2010). Using watershed water balance to evaluate the accuracy of eddy covariance evaporation
530 measurements for three semiarid ecosystems. *Agricultural and Forest Meteorology*, 150(2), 219-225.
531 doi:<https://doi.org/10.1016/j.agrformet.2009.11.002>
- 532 Scott, R. L., Biederman, J. A., Hamerlynck, E. P., & Barron-Gafford, G. A. (2015). The carbon balance pivot point
533 of southwestern U.S. semiarid ecosystems: Insights from the 21st century drought. *Journal of Geophysical
534 Research: Biogeosciences*, 120(12), 2612-2624. doi:<https://doi.org/10.1002/2015JG003181>
- 535 Scott, R. L., Jenerette, G. D., Potts, D. L., & Huxman, T. E. (2009). Effects of seasonal drought on net carbon
536 dioxide exchange from a woody-plant-encroached semiarid grassland. *Journal of Geophysical Research:
537 Biogeosciences*, 114(G4). doi:<https://doi.org/10.1029/2008JG000900>
- 538 Serrano-Ortiz, P., Domingo, F., Cazorla, A., Were, A., Cuevva, S., Villagarcía, L., . . . Kowalski, A. S. (2009).
539 Interannual CO₂ exchange of a sparse Mediterranean shrubland on a carbonaceous substrate. *Journal of
540 Geophysical Research: Biogeosciences*, 114(G4). doi:<https://doi.org/10.1029/2009JG000983>
- 541 Shi, P., Sun, X., Xu, L., Zhang, X., He, Y., Zhang, D., & Yu, G. (2006). Net ecosystem CO₂ exchange and
542 controlling factors in a steppe—Kobresia meadow on the Tibetan Plateau. *Science in China Series D: Earth
543 Sciences*, 49(2), 207-218. doi:10.1007/s11430-006-8207-4
- 544 Stocker, B. D., Wang, H., Smith, N. G., Harrison, S. P., Keenan, T. F., Sandoval, D., . . . Prentice, I. C. (2020). P-
545 model v1. 0: an optimality-based light use efficiency model for simulating ecosystem gross primary
546 production. *Geoscientific Model Development*, 13(3), 1545-1581.

- 547 Sulman, B. N., Desai, A. R., Cook, B. D., Saliendra, N., & Mackay, D. S. (2009). Contrasting carbon dioxide fluxes
548 between a drying shrub wetland in Northern Wisconsin, USA, and nearby forests. *Biogeosciences*, 6(6),
549 1115-1126. doi:10.5194/bg-6-1115-2009
- 550 Suni, T., Rinne, J., Reissell, A., Altimir, N., Keronen, P., Rannik, U., . . . Vesala, T. (2003). Long-term
551 measurements of surface fluxes above a Scots pine forest in Hyytiala, southern Finland, 1996-2001. *Boreal
552 Environment Research*, 8(4), 287-301.
- 553 Syed, K. H., Flanagan, L. B., Carlson, P. J., Glenn, A. J., & Van Gaalen, K. E. (2006). Environmental control of net
554 ecosystem CO₂ exchange in a treed, moderately rich fen in northern Alberta. *Agricultural and Forest
555 Meteorology*, 140(1-4), 97-114.
- 556 T., M. (2016). *FLUXNET2015 US-Goo Goodwin Creek*. Retrieved from FluxNet; NOAA/ARL:
- 557 Tang, B., Zhao, X., & Zhao, W. (2018). Local effects of forests on temperatures across Europe. *Remote Sensing*,
558 10(4), 529.
- 559 Tang, X., Zhou, Y., Li, H., Yao, L., Ding, Z., Ma, M., & Yu, P. (2020). Remotely monitoring ecosystem respiration
560 from various grasslands along a large-scale east–west transect across northern China. *Carbon Balance and
561 Management*, 15, 1-14.
- 562 Tatarinov, F., Rotenberg, E., Maseyk, K., Ogée, J., Klein, T., & Yakir, D. (2016). Resilience to seasonal heat wave
563 episodes in a Mediterranean pine forest. *New Phytologist*, 210(2), 485-496.
564 doi:<https://doi.org/10.1111/nph.13791>
- 565 TEDESCHI, V., REY, A., MANCA, G., VALENTINI, R., JARVIS, P. G., & BORGHETTI, M. (2006). Soil
566 respiration in a Mediterranean oak forest at different developmental stages after coppicing. *Global change
567 biology*, 12(1), 110-121. doi:<https://doi.org/10.1111/j.1365-2486.2005.01081.x>
- 568 Thomas, C. K., Law, B. E., Irvine, J., Martin, J. G., Pettijohn, J. C., & Davis, K. J. (2009). Seasonal hydrology
569 explains interannual and seasonal variation in carbon and water exchange in a semiarid mature ponderosa
570 pine forest in central Oregon. *Journal of Geophysical Research: Biogeosciences*, 114(G4).
571 doi:<https://doi.org/10.1029/2009JG001010>
- 572 Thum, T., Aalto, T., Laurila, T., Aurela, M., Kolari, P., & Hari, P. (2007). Parametrization of two photosynthesis
573 models at the canopy scale in a northern boreal Scots pine forest. *Tellus Series B-Chemical and Physical
574 Meteorology*, 59(5), 874-890. doi:10.1111/j.1600-0889.2007.00305.x
- 575 Tirone, G., Dore, S., Matteucci, G., Greco, S., & Valentini, R. (2003). Evergreen Mediterranean Forests. Carbon and
576 Water Fluxes, Balances, Ecological and Ecophysiological Determinants. In R. Valentini (Ed.), *Fluxes of
577 Carbon, Water and Energy of European Forests* (pp. 125-149). Berlin, Heidelberg: Springer Berlin
578 Heidelberg.
- 579 Turner, D., Ritts, W., Styles, J., Yang, Z., Cohen, W., Law, B., & Thornton, P. (2006). A diagnostic carbon flux
580 model to monitor the effects of disturbance and interannual variation in climate on regional NEP. *Tellus B:
581 Chemical and Physical Meteorology*, 58(5), 476-490.
- 582 Ulke, A. G., Gattinoni, N. N., & Posse, G. (2015). Analysis and modelling of turbulent fluxes in two different
583 ecosystems in Argentina. *International Journal of Environment and Pollution*, 58(1-2), 52-62.
- 584 Urbanski, S., Barford, C., Wofsy, S., Kucharik, C., Pyle, E., Budney, J., . . . Munger, J. W. (2007). Factors
585 controlling CO₂ exchange on timescales from hourly to decadal at Harvard Forest. *Journal of Geophysical
586 Research: Biogeosciences*, 112(G2). doi:<https://doi.org/10.1029/2006JG000293>

- 587 VALENTINI, R., De ANGELIS, P., MATTEUCCI, G., MONACO, R., DORE, S., & MUCNOZZA, G. E. S.
588 (1996). Seasonal net carbon dioxide exchange of a beech forest with the atmosphere. *Global change*
589 *biology*, 2(3), 199-207. doi:<https://doi.org/10.1111/j.1365-2486.1996.tb00072.x>
- 590 Valentini, R., Matteucci, G., Dolman, A. J., Schulze, E. D., Rebmann, C., Moors, E. J., . . . Jarvis, P. G. (2000).
591 Respiration as the main determinant of carbon balance in European forests. *Nature*, 404(6780), 861-865.
592 doi:10.1038/35009084
- 593 Veenendaal, E. M., Kolle, O., & Lloyd, J. (2004). Seasonal variation in energy fluxes and carbon dioxide exchange
594 for a broad-leaved semi-arid savanna (Mopane woodland) in Southern Africa. *Global change biology*,
595 10(3), 318-328.
- 596 Vickers, D., Thomas, C., Pettijohn, C., Martin, J. G., & Law, B. (2012). Five years of carbon fluxes and inherent
597 water-use efficiency at two semi-arid pine forests with different disturbance histories. *Tellus B: Chemical*
598 *and Physical Meteorology*, 64(1), 17159. doi:10.3402/tellusb.v64i0.17159
- 599 Vitale, L., Di Tommasi, P., D'Urso, G., & Magliulo, V. (2016). The response of ecosystem carbon fluxes to LAI and
600 environmental drivers in a maize crop grown in two contrasting seasons. *International Journal of*
601 *Biometeorology*, 60(3), 411-420. doi:10.1007/s00484-015-1038-2
- 602 Wang, S., Ibrom, A., Bauer-Gottwein, P., & Garcia, M. (2018). Incorporating diffuse radiation into a light use
603 efficiency and evapotranspiration model: An 11-year study in a high latitude deciduous forest. *Agricultural*
604 *and Forest Meteorology*, 248, 479-493.
- 605 Wharton, S., Falk, M., Bible, K., Schroeder, M., & Paw U, K. T. (2012). Old-growth CO₂ flux measurements reveal
606 high sensitivity to climate anomalies across seasonal, annual and decadal time scales. *Agricultural and*
607 *Forest Meteorology*, 161, 1-14. doi:<https://doi.org/10.1016/j.agrformet.2012.03.007>
- 608 Williams, M., Law, B. E., Anthoni, P. M., & Unsworth, M. H. (2001). Use of a simulation model and ecosystem
609 flux data to examine carbon–water interactions in ponderosa pine. *Tree physiology*, 21(5), 287-298.
610 doi:10.1093/treephys/21.5.287
- 611 Wohlfahrt, G., Hammerle, A., Haslwanter, A., Bahn, M., Tappeiner, U., & Cernusca, A. (2008). Seasonal and inter-
612 annual variability of the net ecosystem CO₂ exchange of a temperate mountain grassland: Effects of
613 weather and management. *Journal of Geophysical Research: Atmospheres*, 113(D8).
- 614 Wolf, S., Eugster, W., Ammann, C., Häni, M., Zielis, S., Hiller, R., . . . Buchmann, N. (2013). Contrasting response
615 of grassland versus forest carbon and water fluxes to spring drought in Switzerland. *Environmental*
616 *Research Letters*, 8(3), 035007.
- 617 Xiao, X., Hollinger, D., Aber, J., Goltz, M., Davidson, E. A., Zhang, Q., & Moore III, B. (2004). Satellite-based
618 modeling of gross primary production in an evergreen needleleaf forest. *Remote sensing of environment*,
619 89(4), 519-534.
- 620 Xu, T., & Hutchinson, M. (2011). ANUCLIM version 6.1 user guide. *The Australian National University, Fenner*
621 *School of Environment and Society, Canberra*.
- 622 Yee, M. S., Pauwels, V. R., Daly, E., Beringer, J., Rüdiger, C., McCabe, M. F., & Walker, J. P. (2015). A
623 comparison of optical and microwave scintillometers with eddy covariance derived surface heat fluxes.
624 *Agricultural and Forest Meteorology*, 213, 226-239.
- 625 Zhang, J.-H., Han, S.-J., & Yu, G.-R. (2006). Seasonal variation in carbon dioxide exchange over a 200-year-old
626 Chinese broad-leaved Korean pine mixed forest. *Agricultural and Forest Meteorology*, 137(3), 150-165.
627 doi:<https://doi.org/10.1016/j.agrformet.2006.02.004>

628 Zielis, S., Etzold, S., Zweifel, R., Eugster, W., Haeni, M., & Buchmann, N. (2014). NEP of a Swiss subalpine forest
629 is significantly driven not only by current but also by previous year's weather. *Biogeosciences*, 11(6), 1627-
630 1635.

631